UiT
THE ARCTIC
UNIVERSITY
OF NORWAY

Faculty of Health Sciences,

Department of Medical Biology

'miR-126 as a prognostic marker in non-GIST soft tissue sarcoma'

Magnus Persson

Master thesis in Medical Laboratory, MBI-3905. April 2014

Norwegian Translational Cancer Research Center

Population – Bedside – Bench - and back

UNIVERSITY OF TROMSØ

I Acknowledgement

The present work was carried out at the Faculty of Health Sciences, Department of Medical Biology (IMB), as a part of the sarcoma project of the Norwegian Translational Cancer Research Center (NOTCH).

First I want to thank professor and pathologist Lill-Tove Busund who introduced me into the field of research and for encouraging me to take this master thesis. In the establishment of the NOTCH group (former name; Translational Cancer Research Group, UiT) in 2004 she asked me to be responsible for the construction of Tissue Micro Arrays (TMAs) from archived biopsies. I became interested in her offer to be a part of a research group and since then I have produced TMAs for different tumor types in several projects.

I want to thank my supervisor Thomas Berg, hospital scientist, for his expertise in molecular biology. His excellent guidance of the study has been of great importance for me during the work. I also want to thank my co-supervisors, Lill-Tove Busund and professor and oncologist Tom Dønnem for the knowledge they have contributed. Tom Dønnem has been very helpful with the statistical evaluation of the generated data.

I want to say many thanks to engineer Mona Pedersen for her assistance during the performance of miRNA ISH staining, and to pathologist Andrej Valkov for being my co-scorer of the stained specimens. Pathologist Sveinung Sørbye has taking the images of the miRNA stained material used in the study, and illustrator Roy Lysså has made the composition of the images. Thank you to you.

I want to thank the management of the Department of Clinical Pathology, UNN, including the leaders Tor-Arne Hansen and Kate Myräng, that allowed me to combine study with work.

And finally, I want to thank the ladies at the section of cytology for doing my job when I have been off for lectures and lab work.

II List of abbreviations

A	Adenosine
ADAR	Adenosine deaminases act on RNA
Ago2	Argonaute 2
C	Control
CLL	Chronic Lymphocytic Leukemia
DFS	Dermatofibrosarcoma
DGCR8	DiGeorge syndrome critical region 8
DSS	Disease-specific survival
EC	Endothelial cells
Egfl7	EGF-like domain-containing protein 7
Ets	E26 Transformation-specific Sequence
FFPE	Formalin-fixed paraffin embedded
FGF	Fibroblast growth factor
FISH	Fluorescence *in situ* hybridization
H&E	Hematoxylin and Eosin
I	Inosine
IHC	Immunohistochemistry
IMB	Department of Medical Biology
ISH	*In situ* hybridization
KM	Kaplan-Meier
LMS	Leiomyosarcoma
LNA	Locked Nucleic Acid
LOH	Loss of heterozygosity
MM	Malignant mesothelioma
MFH	Malignant fibrous histiocytoma
miRNA	micro RNA (ribonucleic acid)
mi-RISC	miRNA-induced silencing complex
MTA-1	Manual Tissue Arrayer, Beecher instruments
non-GIST STS	non-GIST (gastrointestinal stromal tumor) soft tissue sarcoma
nt	Nucleotides
pri-miRNA	Primary miRNA
RBI1	Recipient block indexer
RMS	Rhabdomyosarcoma
RNA pol II/III	RNA polymerase II/III
RT	Room temperature
SCS	Spindle cell sarcoma
S-MED	Sarcoma-miRNA Expression Database
SNP	Single-nucleotide polymorphism
SPSS	Statistical Product and Service Solutions
SS	Synovial sarcoma
T_m	Melting temperature
TMA	Tissue Micro Array
UiT	University in Tromsø
UNN	University Hospital in Northern Norway
VEGF	Vascular endothelial growth factor
WHO	World Health Organization

III Abstract

Background. MicroRNAs (miRNAs) are a novel class of small non-coding RNA that regulate gene expression in a tissue-specific manner, and consequently, found to be a major factor in tumor development. One of these includes miR-126, a molecular component involved in angiogenesis, and characterized with both tumor suppressor and oncogenic functions.

Purpose. The study aimed to identify prognostic miRNAs in non-GIST soft tissue sarcomas (non-GIST STSs), and to study the impact of miR-126 expression in different subtypes of non-GIST STSs.

Material and Methods. The sample material consisting of 249 formalin-fixed and paraffin-embedded (FFPE) biopsies obtained from the University Hospital in Northern Norway (UNN) and Hospitals in Arkhangelsk County, Russia were arranged in Tissue Micro Array (TMA) cohorts. miRNA screening was performed on samples from two prognostic groups: 1) 11 patients with long disease-specific survival (DSS) and 2) 10 patients with short DSS mainly diagnosed with leiomyosarcoma (LMS) and malignant fibrous histiocytoma (MFH). In addition, normal controls (C) from skin and uterus were included. Microarray-based expression profiling was used for screening the samples for all human, mouse and rat miRNAs registered in miRBase (n=1274). Heat map and unsupervised hierarchical clustering, and volcano plots were used to identify differentially expressed miRNAs.

The prognostic impact of miR-126 in the non-GIST STS population was determined by miRNA *in situ* hybridization (miRNA ISH). ISH stained TMA slides were scanned and digitized by Ariol Imaging System and scored manually using a semi-quantitatively scale. The software package SPSS version 19 was used for statistical analysis.

Results. For long DSS versus control, 47 miRNAs were demonstrating significant dysregulation, and for short DSS versus C, 54 miRNAs were proven to be dysregulated. These miRNAs were mainly repressed. In comparison of long DSS versus short DSS it could not be manifested any prognostic significance in miRNA regulation.

In the total non-GIST STS population there was no statistically significant impact of miR-126 expression. When stratifying into histological subgroups, however, miR-126 became a strong positive prognostic factor in LMS. The prognostic impact of non-uterus LMS was rather striking; none of the nine patients with high miR-126 expression died of their sarcomas, while none of the 14 patients with low miR-126 expression survived ($p<0.001$).

Conclusion. The study demonstrated significant deregulation of miRNAs in sarcomas, and miR-126 was indicated to be a crucial factor for survival rate in LMS.

Contents

1 Introduction

1.1 Cancer

Cancer is abnormal growth of cells which can start in any part of the body. There are more than 100 types of cancers classified according to organ and cells involved [1].

It is a genetic disease caused by accumulation of gene mutations arising in a limited group of cells. Altered DNA sequences in genes may change the nature of cells, which later could culminate in formation of malignant tumor [2].

It is established six hallmarks to describe the biological behavior of cancer diseases (Figure 1) [3]. The most important feature of malignant cells is unlimited proliferation without control from external stimulus. The ability of tumors to invade surrounding tissues and spread to other organs is often the fatal factors for the outcome of the disease.

Morphologically, the tumor cells are characterized by enlarged and abnormal nuclei [4]. The nucleus is hyperchromatic because of increased DNA activity, and mitoses are frequently seen as a consequence of enhanced proliferation.

Cancers are commonly categorized into five main groups based on cells of origin [5]. The largest group comprises carcinomas derived from epithelial tissue and involves organs such as, lungs, breast, prostate, pancreas and the gastrointestinal tract (GIST). The other groups comprise; sarcomas originating in connective tissues, lymphomas arising in lymphatic cells, leukemia involving cells of the blood system, and melanoma affecting the cells making the pigment in the skin. Age is the most important risk factor for getting cancer. Other known causes include the family history, tobacco, sunlight, chemicals, ionizing radiation, and infectious agents [6]. Human cancer is one of the leading death causes worldwide, and according to World Health Organization (WHO) almost eight million people die per year [7].

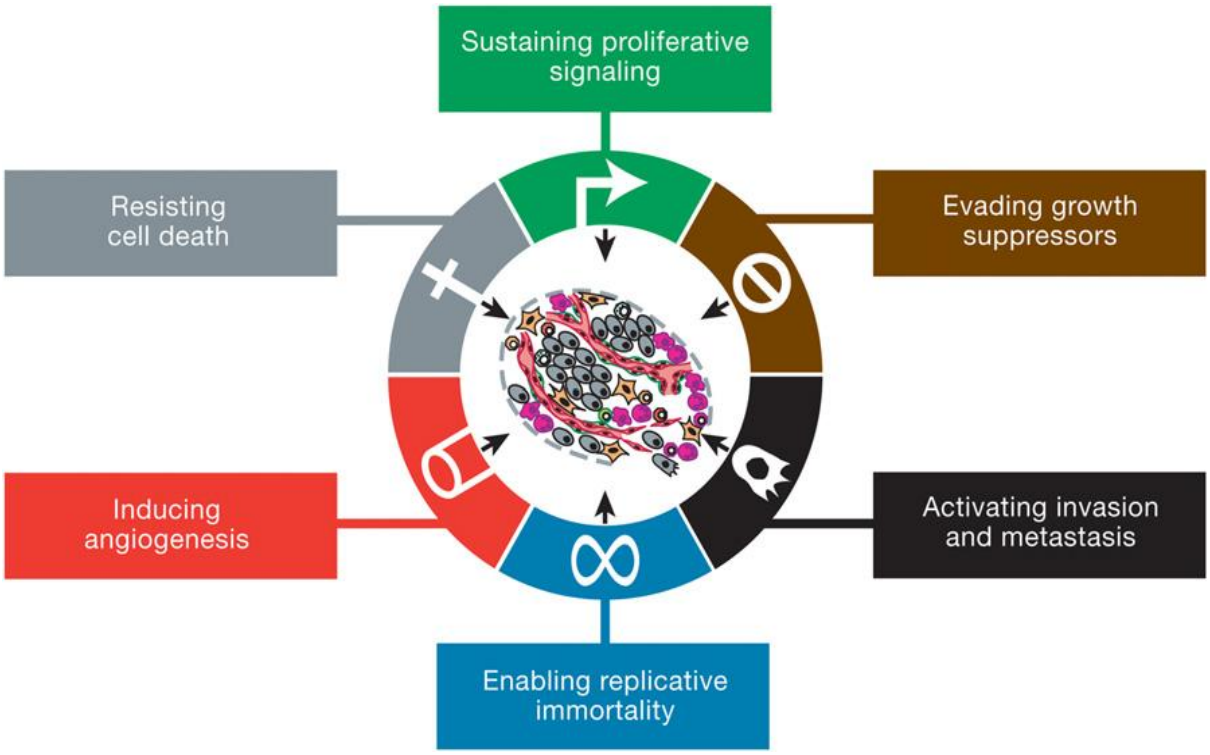

Figure 1. The six hallmarks of cancer defined by Hanahan and Weinberg (2011). These features describe the underlying mechanisms in development of cancer [3].

1.2 Sarcoma

Sarcoma, derived from the Greek *sarx*, meaning flesh, is a form of cancer involving the connective tissue [8]. It is a rare malignancy, representing about 1% of cancers in adults, and in children and adolescents the proportion is 15% [9]. Sarcoma represent a heterogenous group of malignancies, and based on histological characteristics the sarcoma tumors are classified into two main groups, soft tissue sarcomas (STSs) and bone sarcomas. STSs consist of 50 histological subtypes, whereas 20 types are found in bone sarcomas [9]. STSs arise in tissues like blood vessels, fat, muscle, nerves, and tendons, and classified in accordance with their histological differentiation [10]. Tables 1 and 2 list some of the common types of sarcomas [11].

Table 1. Common types of bone sarcomas

Bone sarcoma types	Connective tissue of origin
Chondrosarcoma	Cartilage
Ewing sarcoma	Bone (usually in young patients)
Osteosarcoma	Bone
Rhabdomyosarcoma (RMS)	Skeletal muscle (children)

Table 2. Common types of soft tissue sarcomas (STSs)

Soft tissue sarcoma types	Connective tissue of origin
Angiosarcoma	Blood and lymph vessels
Fibrosarcoma	Fibrous tissue
Gastro-intestinal stromal tumor (GIST)	Neuromuscular cells of digestive tract
Leiomyosarcoma (LMS)	Smooth muscle tissue
Liposarcoma	Fat tissue
Malignant fibrous histiocytoma (MFH)	Fibrous tissue
Malignant peripheral nerve sheath tumor	Nerves and related tissue of brain and spinal cord
Synovial sarcoma (SS)	Joints

STSs may develop almost anywhere in the body, but are most prevalent in arms and legs (60%). Around 40-45% involve abdominal region and GI-tract, and 9% are localized to head and neck [12] (Figure 2). The age of diagnosis may vary greatly, but the average age is 57 years. The exceptions are Ewing sarcoma and rhabdomyosarcoma (RMS) which are mainly related to children [13]. Sarcoma is evenly distributed across ethnicities, but men seem to be slightly more affected than women [14]. The initial symptoms of STS are usually characterized by a diffuse swelling in the current location, and the tumor must grow considerable before painful symptoms appear [15].

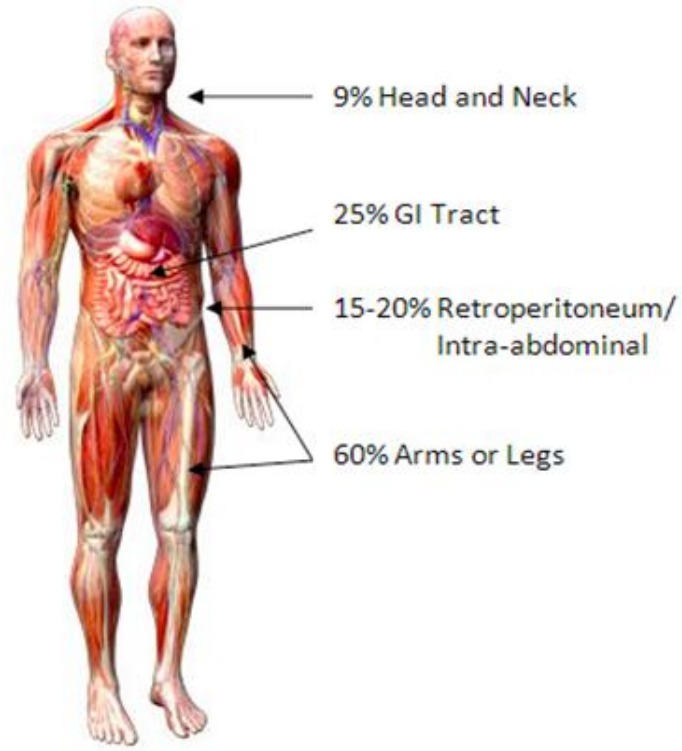

Figure 2. The locations of soft tissue sarcomas (STSs) in the body [12]

1.2.1 Diagnosis

Sarcoma diagnostics is mainly based on imaging tests and histopathological investigation of biopsies. Imaging tests are useful in identifying and locating the tumor, and to determine whether the tumor is benign or malignant. Benign tumors usually consist of a round and well-defined mass, whereas the malignant ones have more ill-defined growth pattern [16].
A biopsy is taken to confirm a definitive sarcoma diagnosis [16]. A portion of the tumor is resected from the body and fixed. At pathological labs the tumor tissue is processed in different steps and finally embedded in paraffin blocks. Thin histological sections are cut and mounted on glass slides, and stained with hematoxylin and eosin (H&E). A pathologist studies the tissue morphology under a microscope to give a diagnosis. The diverse histological features in combination with few cases of sarcomas, often make the diagnosing challenging. Therefore, the basic H&E staining might be supplemented with special tests, in order to rule out differential diagnoses and/or for making correct subtyping.
Immunohistochemistry (IHC) is a well established method to determine from which lineage the cells derives from [17]. A range of antibodies are routinely used in sarcoma diagnostics, and normally a panel of IHC markers is required to give an accurate classification.
In recent years, different subclasses of sarcomas have been characterized with unique molecular alterations that can be used as diagnostic tools [18]. A known example is the Kit- and PDGFRA mutations in GIST. By use of methods, such as fluorescence *in situ* hybridization (FISH) and real-time polymerase chain reaction (PCR) to detect specific genetic alterations associated with STS entities the diagnostics become more specific. A novel approach in molecular studies involves expression profiling of nucleic acids [19]. So far, this technique is mainly used in research to reveal distinct expression patterns of genes/miRNAs to different cancer types. Microarray-based expression profiling will be described section 2.7.

1.2.2 Tumor staging

The extension of a tumor is assessed by the TNM staging system [20]. T indicates the size of the tumor, N possible spread to lymph nodes, and M if there is metastasis to other organs. Each letter is combined with a number, measuring the severity for each variable. Regarding sarcomas, it should be noted that spread to lymph nodes is not common.
Along with the TNM classification, it is established a histological grading system (G) ranging from 1 to 3, describing the aggressiveness based on cellular differentiation [20]. TNM staging and grading (G) are combined to classify the tumors in different prognostic groups (stage I-IV).

1.2.3 Risk factors and treatment

There are no definitive risk factors associated with STS, but exposure for chemicals, such as herbicides and chlorophenols have been reported to increase the risks [21]. Additionally, patients that have undergone radiation therapy for a previous cancer are found to be slightly more predisposed for getting subsequent sarcoma [22].

The treatment strategies are dependent on the type of sarcoma, the stage of the tumor, and the age and health status of the patient [23]. Surgery is the main treatment for low-grade and localized tumors. Radiation therapy could be complemented if there are close margins and also to avoid recurrence of the tumor. Patients having high-grade localized tumors may receive radiation- or chemotherapy prior to surgery to reduce the size of the tumor. Metastatic sarcomas are often treated with a combination of surgery, radiation, and chemotherapy [24]. Patients with GIST can undergo targeted therapy, by use of imatinib which inhibit the tyrosine kinase activity of c-kit [25].

1.2.4 Survival rate

For STSs the overall relative 5-year survival rate is about 50% according to statistics from National Cancer Institute (NCI), US [26]. It indicates the percentage of patients who are alive five years after the time of diagnosis. Those who die from other diseases are excluded.

But the survival rate varies greatly depending on tumor stage at time of detection. For localized sarcomas the 5-year survival rate is 83% for localized sarcomas, 54% for regional stage sarcomas, and 16% for sarcomas with distant spread [26]. Sarcomas in arms and legs usually have better prognosis than more centrally located, and also younger patients seems to have better outcome. Notably, the results for 10-year survival rate are only slightly poorer, indicating that patients living after five years can be considered as cured [26].

1.3 MicroRNA (miRNA)

miRNAs comprise a large group of post-transcriptional gene regulators that have gained considerable attention in the last decade. They represent a class of non-coding RNAs of ~22 nucleotides (nt) that repress gene expression through binding target mRNAs. The effect is either mRNA degradation or suppression of protein translation [27]. The structures of miRNAs are well conserved throughout evolution, and their existence is proven in both animals and plants, indicating their importance in biology [28]. The molecular characteristics of miRNA was described for the first time in 1993 by Victor Ambros, Rosalind Lee and

Rhonda Feinbaum when studying the gene *lin-14* in *C. elegans* development [29], but it was not until the beginning of 2000s miRNAs were defined as a group of molecular components with specific functions [30]. Since then, thousands of miRNAs have been identified across organisms by bioinformatics approaches and experimental works [31], and according to miRBase (http://www.mirbase.org) it is registered 30 424 mature miRNAs in 206 species (Release 20, June 2013) [32]. In the human genome around 1000 miRNAs have been verified, and these are believed to regulate 60% of the protein-coding genes [28, 33]. The miRNA-regulated proteins mainly participate in processes controlling cell fate determination and development, including differentiation, proliferation, apoptosis, and metabolism [29]. The miRNA biogenesis is a multi-step process requiring several essential cofactors to yield optimal levels of mature miRNAs [34]. Moreover, the miRNA synthesis itself is strictly regulated to achieve tissue-specific protein synthesis [34]. Therefore, it is not surprisingly that dysregulated miRNAs have been addressed a major role in human cancers [35].
There are also other small RNA molecules that should not be confused with miRNAs, for instance piwi-interacting RNA (piRNA) and small interfering RNA (siRNA). piRNAs are slightly longer, 26-21 nt, have no sequence conservation, and are more complex [36]. siRNA comprise a group of double stranded RNA molecules with 20-25 base pairs in length which block gene expression through RNA interference [37].

1.3.1 miRNA nomenclature

The miRNAs registered in the miRBase are organized in a standardized nomenclature system [38, 39]. miRNAs are named in the order they are discovered, meaning that for example mir-352 was published before mir-353 [39]. The prefix mir in small letters refers to precursor miRNA (pre-miRNA) and miRNA genes, while the prefix, miR, with a capitalized R refers to mature miRNA [38]. Two pre-miRNAs at specific locus could give rise to two absolutely identical miRNA genes located in different genomic positions. These precursors are termed by adding a dash-number suffix, for example mir-121-1 and mir-121-2. miRNAs exhibiting high sequence similarities are separated by adding a letter exemplified by miR-121a and miR-121b [39]. To distinguish miRNAs originating from different species an initial three letter prefix is used. Thus, human miRNAs are named hsa-miR (homo sapiens)
During miRNA processing mature miRNA duplexes are normally produced by a common pre-miRNA molecule. To separate them, an asterisk is following that miRNA sequence with lowest relative expression. For example, miR-126 is more abundant than miR-126* [38].

1.3.2 Biogenesis of miRNA

Human miRNA genes are found on all chromosomes, except for the Y-chromosome, and located in intergenic regions and in introns of protein-coding genes [40]. Intergenic miRNAs and intronic miRNAs in antisense orientation are transcribed as autonomous units, whereas intronic miRNAs in sense orientation are co-expressed with its host gene [41]. It is also found that closely related miRNAs often are arranged in polycistronic clusters, and transcribed as one unit [40].

miRNAs are normally transcribed by RNA polymerase II (RNA pol II) into primary miRNA transcripts (pri-miRNA), which are 5'capped, polyadenylated, and spliced [28] (Figure 3). Transcription by RNA pol III has also been reported [42]. Thereafter, miRNAs are processed in two subsequent steps by the RNase III enzymes Drosha and Dicer. In the first step, pri-miRNA consisting of hundreds up to thousands of nucleotides folded into hairpins is cleaved precisely by a microprocessor complex, consisting of Drosha and DiGeorge syndrome critical region 8 (DGCR8), to generate pre-miRNA. pre-miRNA comprising a 60-100 nt hairpin structure is transferred from the nucleus to the cytoplasm by Exportin-5 in a Ran-GTP-dependent manner [43, 44].

In the cytoplasm, a second cleavage by Dicer associated with the RNA binding protein TRBP removes the hairpin loop, to form an imperfect ~22 nucleotide miRNA duplex. The two strands are separated, and the one intended to be the functional miRNA is selected by the Argonoute 2 (Ago2) protein for being incorporated into miRISC complex (miRNA-induced silencing complex). This strand is the mature miRNA sequence (miRNA), and referred as the guide strand. The other strand, termed the passenger strand (miRNA*), is degraded [34]. It is thought that thermodynamic properties determine the strand destined to be processed into mature miRNA. In the miRNA:miRNA* duplex, the relative stability at the 5'end of the guide strand is weaker, which favour its integration into the miRISC complex [28].

miRNA incorporated into miRISC guide the complex to target mRNAs, and depending on degree of complementarity, miRNA will either repress protein translation or be degraded (Figure 3) [45]. The binding between miRNA and mRNA is accomplished through perfectly Watson-Crick base pairing between nucleotides 2-8 of the miRNA strand, termed the seed sequence and the untranslated 3'UTR region of matching mRNA [46]. In repression of protein translation, the mature miRNA is characterized by a bulge sequence, leading to partial complementarity to matching mRNA. In contrast, when miRNA:mRNA duplexes exhibiting perfect complementarity, the mature miRNA is cleaved and degraded [27, 46]. In this way, miRNAs fine-adjust the protein synthesis in a highly tissue-specific manner. The complexity

of miRNAs is also confirmed by the fact that each miRNA can regulate hundreds mRNAs, and conversely, several mRNAs can coordinately regulate a single miRNA [44].

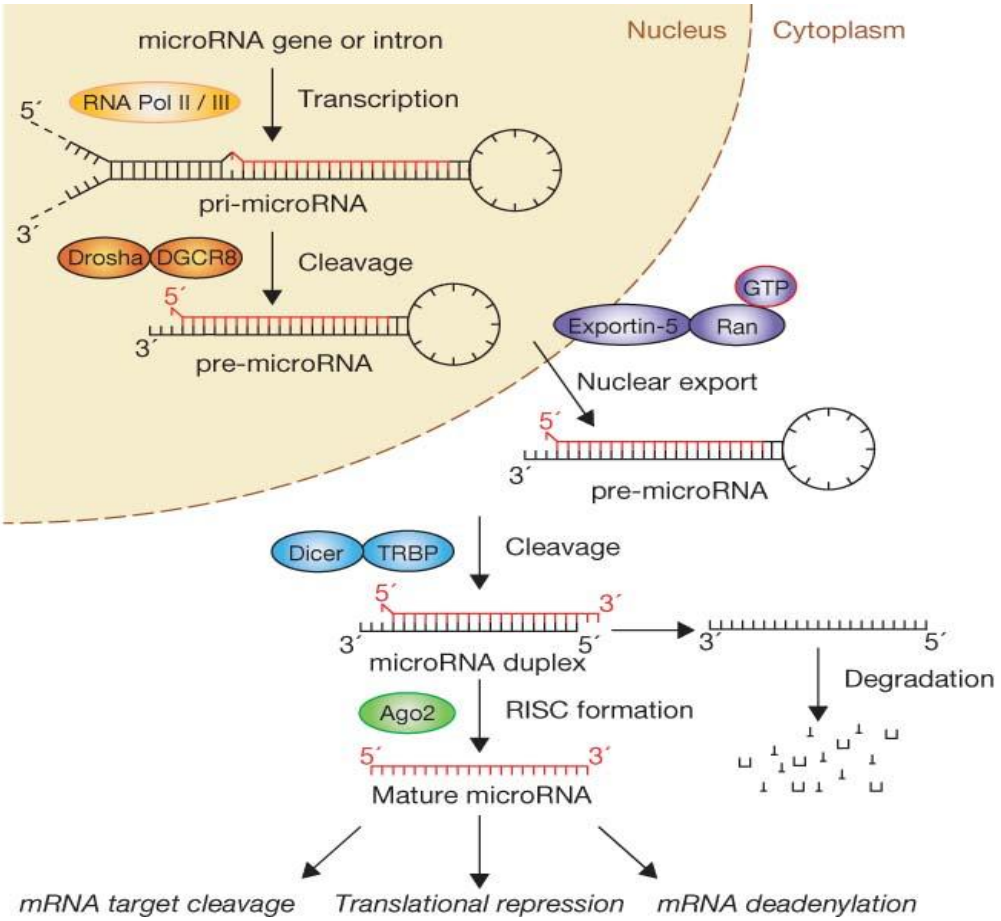

Figure 3. miRNA biogenesis. miRNA genes are transcribed by RNA pol II/III into pri-miRNA and enzymatically cleaved by Drosha/DGCR8 complex into pre-miRNA. The pre-miRNA hairpin structure is transferred from the nucleus to the cytoplasm with help of Exportin-5 where it is cleaved by Dicer into ~22 nt miRNA duplex. The double-stranded miRNA is unwounded and the passenger strand is degraded. The mature miRNA joins the miRNA-induced silencing complex (miRISC) and guide miRISC to target mRNAs to induce gene silencing. Based on degree of complementarity of the miRNA/mRNA complex the proteins synthesis will be either blocked or repressed [42].

1.3.3 Regulation of miRNA biogenesis

The important role of miRNAs in cellular networks requires a strictly controlled miRNA biogenesis. It involves coordinated regulation of miRNA synthesis at different steps, involving several RNA binding cofactors [34].

Transcription

Control of miRNA gene transcription is the first major step in miRNA processing. Transcription factors (TFs) and miRNAs often operate closely together in regulatory

networks, to either activate or repress expression of miRNAs. Autoregulatory feedback loops is a common mechanism, in which miRNAs target mRNAs that produce TFs acting on the same miRNAs, and thereby, miRNAs are able to regulate their own transcription [47]
It is also evident that TFs and miRNAs form genetic circuits where single TFs regulate distinct groups of miRNAs that in turn bind downstream TF-miRNA partners [29]
The importance of TF-miRNA partners in control of physiological processes has led to establishment of a TF-miRNA regulation database, named TransmiR http://cmbi.bjmu.edu.cn/transmir [48, 49].

Drosha processing

During miRNA processing, the levels of the microprocessor proteins Drosha and DGCR8 are stringently regulated through an autoregulatory feedback circuit (Figure 4) [50]. In the crossregulation, Drosha repress DGCR8 synthesis by cleavage of hairpins of the DGCR8 mRNA. DGCR8 in turn, positively regulate Drosha through protein stabilization. For precise cleavage of pri-miRNA, it is of particularly importance that the ratio of the microprocessor components is tightly linked. In a sizeable number of miRNAs, the two RNA helicases, p68 and p72, are included in the Drosha-DGCR8 complex to provide accurate pri-miRNA processing [34].

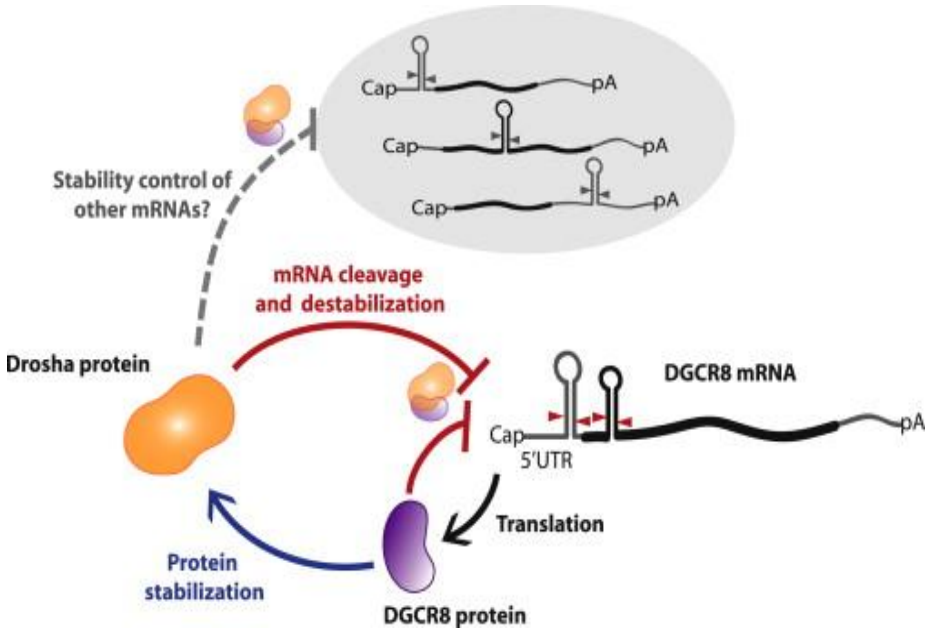

Figure 4. The Drosha and DGCR8 autoregulatory feedback system. Raised levels of Drosha repress DGCR8 mRNA, and translation into DGCR8 protein. This lead to destabilization of the Drosha protein and downregulation of the microprocessor activity in miRNA biogenesis [50].

Dicer- and miRSC processing

The Dicer processing of pre-miRNA appears to be an effectively regulated process, since the relative amount of pre-miRNA is lower than that for pri-miRNA and mature miRNA [28]. The level of Dicer is closely controlled by its cofactor TRBP. Reduced amount of TRBP results in Dicer instability and inhibition of pre-miRNA processing. In addition to pre-miRNA cleavage, Dicer assists Ago2 in loading the mature miRNA into miRISC [47]. Ago2 levels in turn is tightly controlled to mediate cell-type specific mRNA silencing [34].

RNA editing

RNA editing is a miRNA regulation mechanism, in which adenosine (A) is converted into inosine (I) by means of adenosine deaminases act on RNA (ADAR). miRNA regulation through RNA editing normally takes place on double-stranded miRNA intermediates [51]. Altered structure of miRNA precursors through RNA modification could result in both positive and negative stimulation of miRNA processing. If editing occur within the seed sequence of miRNA, it can lead to change of mRNA targets [47].

Epigenetic mechanisms

Epigenetic mechanisms, well-known to regulate protein-coding genes, have also been linked to miRNA regulation. Epigenetics, such as DNA methylation and histone modifications are proved to regulate the expression of a subset of miRNAs [52]. DNA methylation, restricted to CpG islands in promoter sequences, result in suppressed gene expression, while histone modifications, including histone acetylation promote gene transcription. It is assumed that these processes are linked together to regulate protein translation. Vice versa, miRNAs are shown to regulate epigenetic processes, meaning that epigenetics and miRNAs are able to form intricate networks controlling gene expression at transcriptional and posttranscriptional levels [53].

1.4 miRNA and cancer

miRNA was early proposed a role in human cancer based on finding indicating crucial involvement in tissue-specific gene regulation. Moreover, it was shown that miRNA genes tend to be restricted to genomic regions of chromosomal abnormality, associated with malignant transformation [54].

The first evidence of miRNA as a contributing factor in tumor development was reported in 2002. Calin et al. then demonstrated aberrant expression of miR-15 and miR-16 in chronic lymphocytic leukemia (CLL). These miRNAs were found to be located in the 30-kb deletion region of chromosome 13, the main diagnostic criteria of CLL. In CLL miR-15 and miR-16 are lower expressed in 68% of the cases, supporting a critical role in lymphatic pathogenesis [55].

Since then, experimental profiling methods have revealed a significant number of miRNAs coupled to cancers [56]. Mostly, miRNAs are lower expressed in tumor tissue than in corresponding normal tissue, indicating that tumor suppressor features are more dominant than oncogenic features [57]. A common name for these cancer-associated miRNAs are oncomirs [58].

Aberrant miRNA processing can be explained by alterations in the miRNA gene sequence, epigenetic mechanisms, and/or inhibited miRNA processing. As miRNA genes frequently are located in regions of genomic instability they are susceptible for chromosomal rearrangemants, which could give rise to pathological conditions [35]. For example, in loss of heterozygosity (LOH) a tumor suppressor gene can be deleted. In fragile sites, a variety of sequence alterations are prone to happen, including sister chromatid exchange, translocation, amplification, deletion, or incorporation of tumor-associated viruses. Notably, miRNA is not as vulnerable to single-nucleotide polymorphism (SNP) as mRNA [35].

Considering epigenetic mechanisms there are reports describing silencing of miRNAs due to DNA hypermethylation of CpG islands in promoter sequences in different malignancies [59]. Defects in miRNA processing leading to global reduction of miRNAs in tumor tissues have been demonstrated through experimental knockdown of the key enzymes, Drosha and Dicer, in human cancer cell lines. A study by Kumar et al. in 2008 clearly indicated global loss of miRNAs in malignant cells, and aberrant tumor growth in vitro [55]. Moreover, it appears that that the level of miRNA expression correlates with degree of tumor differentiation [55].

1.5 miRNA-126 (miR-126)

In the current study it was decided to focus on the expression of miR-126 in sarcomas. The rationale for selecting miR-126 was based on its proved impact in various cancers. Experimental methods describe loss of miR-126 in cancerous tissue, and through miR-126 transfection malignant growth is considerably reduced, thus indicating its potential as a tumor suppressor. [60-62]. Regarding the significance of miR-126 in sarcomas there are few

published studies, and it was therefore determined to explore its effect in a large patient cohort of different sarcoma subtypes.

Basically, miR-126 is known as a key regulator of angiogenesis in various body tissues, predominantly in highly vascularised organs, such as heart and lung [63]. It is enriched in endothelial cells (ECs) and hematopoietic stem cells, where it serves several angiogenic processes, including embryogenesis, menstruation, and wound healing [61].

miR-126 and its complementary partner miR-126* are located in intron 7 in the *egfl7 gene* (Figure 5) [64]. The *egfl7/miR-126* locus is thought to be co-activated by the common E26 Transformation-specific Sequence (Ets) transcription factor [61, 65]. The Egfl7 protein (EGF-like domain-containing protein 7) and miR-126 are proposed to collaborate closely in formation of new blood vessels, where Egfl7 regulates lumen creation during vasculogenesis, whereas miR-126 is responsible for the angiogenic process and maintenance of the vascular structure [64].

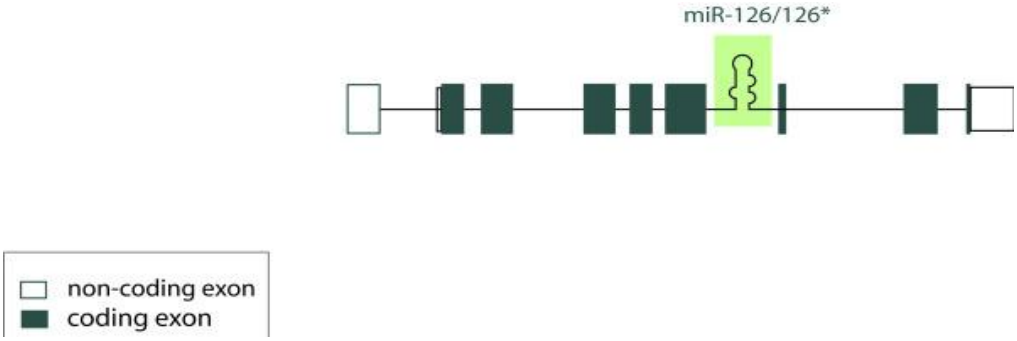

Figure 5. miR-126/126* are located within intron 7 of *egfl7 gene* in all vertebrates [64].

miR-126 promotes vessel formation by blocking Spred-1 and PIK3R2, negative regulators of the MAP kinase and PI3 kinase pathways in ECs (Figure 6). Angiogenesis is induced through binding of vascular endothelial growth factor (VEGF) and fibroblast growth factor (FGF) to EC surface receptors, which activates VEGF signaling leading to downstream expression of genes participating in angiogenesis and vessel integrity [66]. The importance of miR-126 in vascular network stability has been investigated in miR-126 knockdown models. Absence of miR-126 clearly shows repression of angiogenic pathways as a consequence of elevated levels of PIK3R2 and Spred1 [63, 66] . The phenotypic results include defect vascular integrity in terms of impaired vessel formation and ruptured lumens [61].

Regarding the miR-126 partner, miR-126* there is little knowledge about its functional role in relation to miR-126. They are both expressed in the same tissues, but if they are restricted to the same cell lineage, or in the same cells remains unclear. However, it is believed that miR-

126* is not involved in angiogenic mechanisms to the same extent as miR-126, but more act as a tumor suppressor through repression of proliferation, migration, and invasion [61].

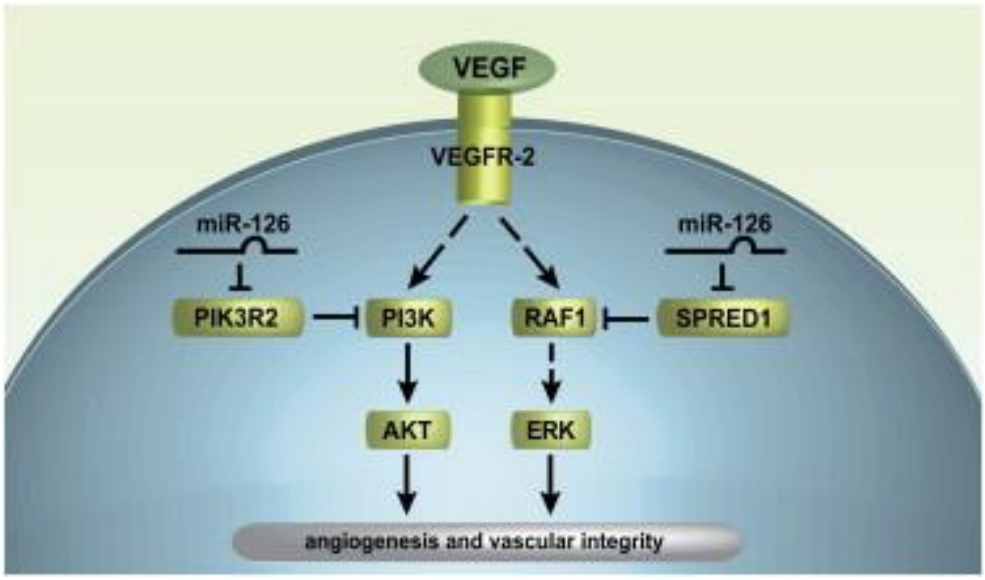

Figure 6. miR-126 control VEGF signaling in ECs through inhibition of the signaling proteins PI3K and RAF1 via negative regulation of the growth factors PIK3R2 and SPRED1. This in turn, trigger the PI3 kinase and MAP kinase pathways culminating in expression of genes involved in angiogenesis and vascular maintenance [66].

Several malignancies have been associated with dysregulated miR-126, but its functional role in tumor development is far from clarified. According to Meister and Schmidt (2010) upregulation of miR-126/miR-126* in tumor vascularity may contribute to neoplastic angiogenesis, resulting in tumor expansion. Downregulation of miR-126/miR-126* in tumor vessels are thought to cause weakened vascular integrity, that in turn drive tumor progression to promote cell proliferation, migration, escape from cell death, and infiltration of leukocytes into lumen. Even greater reduction of miR-126/miR-126* can damage the vascular integrity so seriously that a chaotic tumor vasculature is formed (Figure 7) [61].

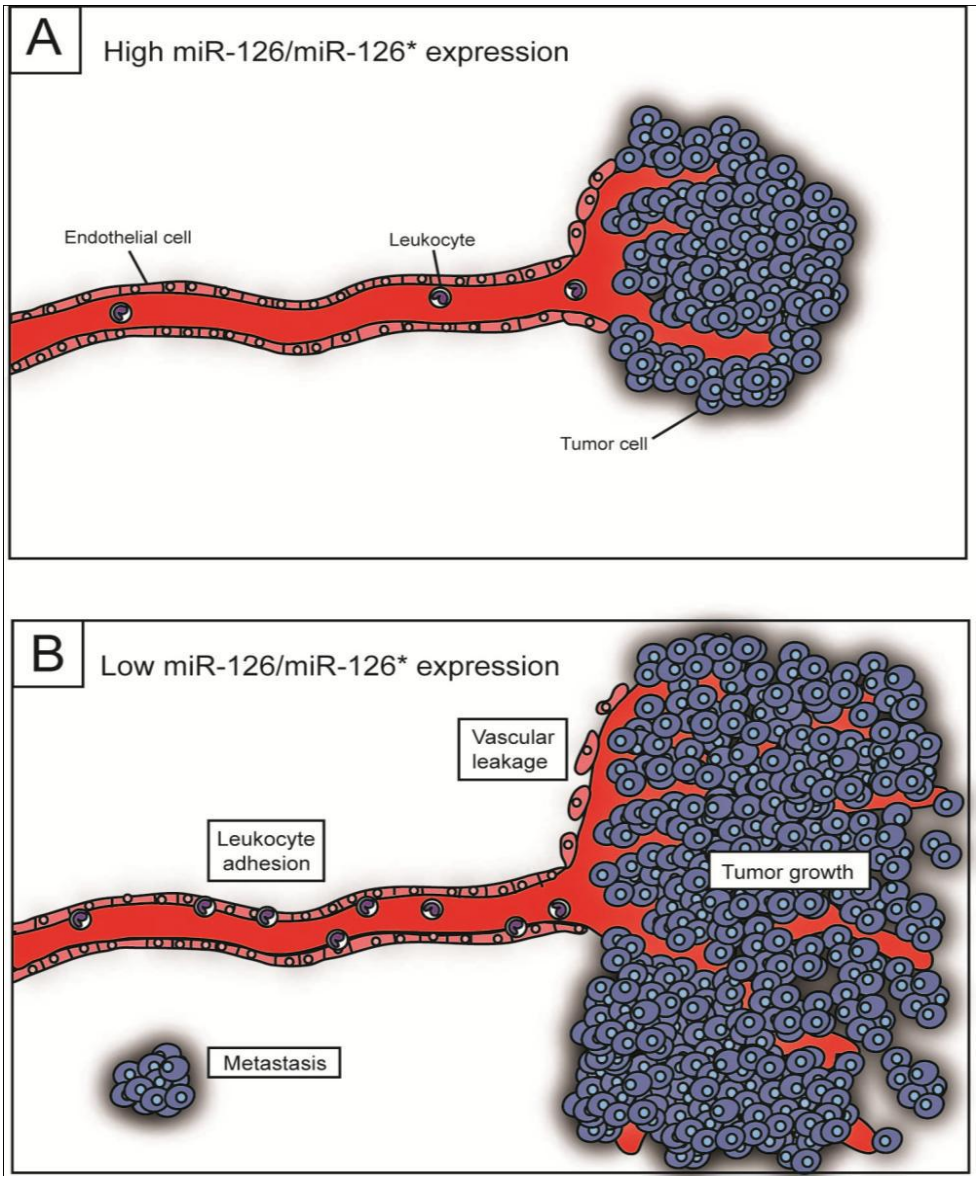

Figure 7. The suggested effects of miR-126/miR-126* deregulation in tumor development. (A) Oncogenic activity by miR-126/miR-126* induce creation of new blood vessels as a result of angiogenic stimulation of endothelial cells. (B) Low expression of miR-126/miR-126* in tumorigenesis is thought to promote cell proliferation, migration, and survival instinct. Also the vascular integrity is affected and may transform into a chaotic and neoplastic vasculature [61].

1.6 Tissue Micro Array (TMA)

Tissue Micro Array (TMA) is based on the idea to assemble small amount of sample material from hundreds of archived tissue blocks (FFPE biopsies) into one single paraffin block (Figure 8) [67]. Tiny tissue cores retrieved from donor blocks are precisely arranged in a grid pattern in the recipient block, termed the TMA block. This innovation was introduced by Battifora H in 1986, who created the "multi-tissue" block. The methodology was further modified by J Kononen through the launch of a commercial tissue microarray (Manual Tissue Array (MTA-1), see section 2.6.1), Beecher Instruments, Sun Prairie, WI, US in 1998 [68].

From TMA blocks thin histological sections are cut with a microtome and mounted on glass slides. TMAs applied in IHC staining and *in situ* hybridizations (ISH and FISH) provide high-throughput analyzing of large sample material under standardized and identical conditions [67, 68]. The methodology has been successfully introduced into translational cancer research for identification of biomarkers important in tumor-specific progression. Significant findings in studies enable implementation of more effective diagnostics and better prognosis [67, 68].

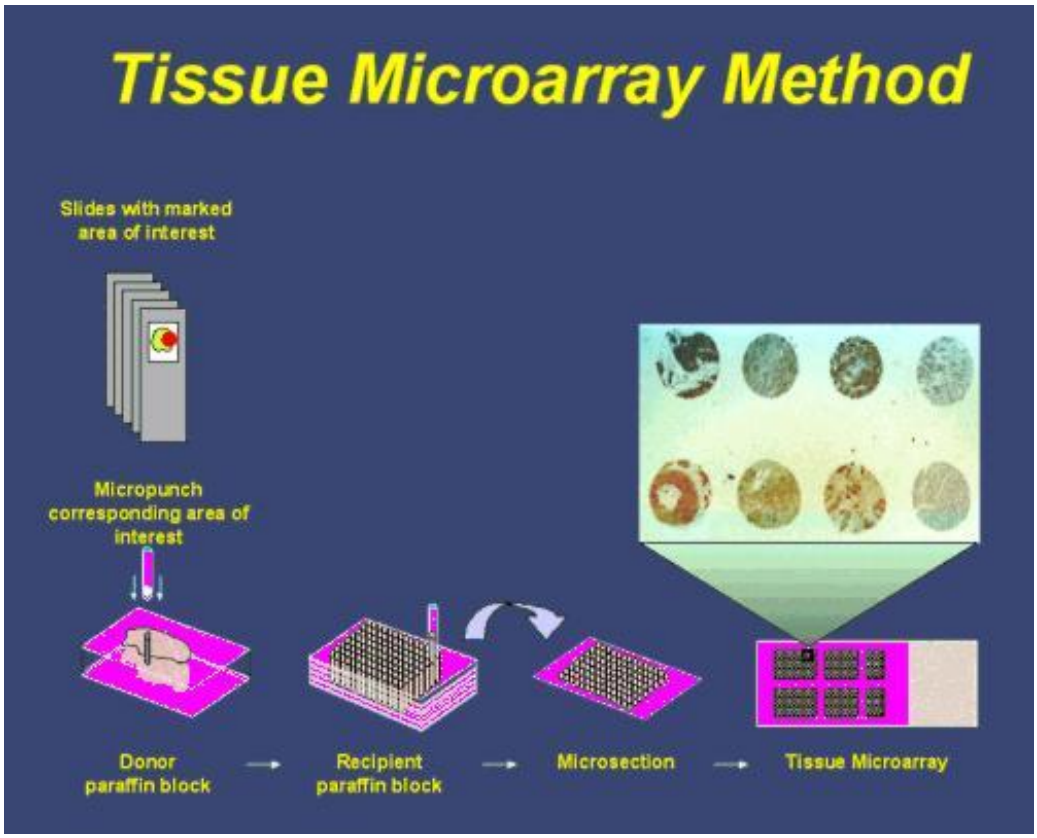

Figure 8. Tissue Micro Array (TMA) construction. Biopsies and associated H&E slides are collected from histological archives. Area of interest for the H&E slide are marked. Tissue cores (normally 0.6mm) are punched from the corresponding area on the donor blocks (FFPE biopsies), and placed into the pre-made cores of the recipient block. A recipient block containing donor cores in defined positions constitute TMA block. Microsections are cut to be used in downstream analyzing. Unique array patterns for TMAs are recommended for easy orientation [69].

1.6.1 Manual Tissue Array (MTA-1) instrument

The instrument, MTA-1, used for TMA construction is a mechanical device with manual operating procedures (Figure 9). Four recipient blocks are attached in a rotating block holder (recipient block indexer (RBI1)). The switching turret seen in front of the MTA-1 has two positions for punch needles. The first one, termed the recipient needle, is intended for creating empty cores in the recipient block, and the second and somewhat larger one, termed the donor needle, is used for extracting tissue cores from donor blocks, which are then placed into the

pre-made holes of the recipient blocks. The needles are navigated by X-Y micrometers with an accuracy of 0.001mm. A recipient block containing array sections of tissue cores is referred as a TMA block. Use of a rotating block holder enables simultaneous creation of four identical TMA blocks, thereby more material for downstream analysis is obtained [70].
The MTA-1 instrument can also be applied for dissection of tissue material for nucleic acid extraction. By using a punch needle, tissue cores from selected regions of FFPE biopsies are removed and collected into eppendorf tubes [70].

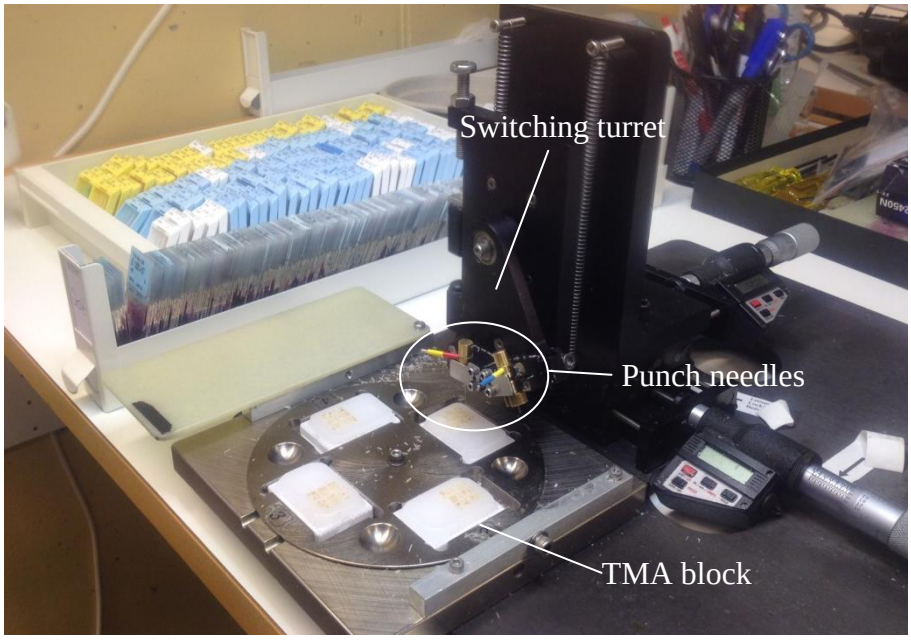

Figure 9. TMA construction using Manual Tissue Arrayer (MTA-1), Beecher Instruments. MTA-1 is a manually operating instrument consisting of a block holder positioned on the base plate, and above, there is a switching turret holding the recipient and donor punches. The punches are moved by the X-Y micrometers with an accuracy of 0.001mm. Donor blocks and corresponding H&E slides are seen on the left hand of the instrument. The TMA working station at IMB, UiT.

1.6.2 Practical aspects of TMA construction

Tissue microarray has become a powerful and informative research tool to explore expression profiles for biomarkers involved in pathogenesis of different diseases. Using TMA sections for molecular analyzes dramatically reduce the labor time and the costs relative to single-slide assays. By using 0.6mm punching needles it will be minimal damage to the donor blocks [71]. Analysis of TMA material requires array blocks of good quality. Cares should be taken to pushing down the cores at the same level and allow them to homogenize with the surrounding paraffin. It is also recommended to arrange an irregular TMA layout for easy orientation for persons involved in the study.

1.7 Microarray-based expression profiling of miRNA

miRNA screening was performed on two prognostic groups of non-GIST STS based on long and short time of survival. The aim was to identify miRNAs significant for survival of the disease. Total-RNA was isolated from a selected number of samples included in the total patient cohort. Expression profiling of the samples was outsourced to Exiqon, Denmark.

1.7.1 Global miRNA expression profiling

Expression profiling is a powerful tool to elucidate the functional role of nucleic acids in biological processes [72]. It is based on the microarray technology providing parallel analysis of hundreds up to thousands of molecular markers in a single assay [73]. The method was initially developed for gene expression profiling in the 1980s [74]. In the past decade, expression profiling of miRNAs has gained impact in cancer research, where studies have characterized different tumors with unique miRNA phenotypic signatures [75]. Normally, the goal of miRNA profiling is to compare the relative expression between two physiological conditions, for example, disease versus normal state, in order to identify markers with pathogenic relevance [76].

miRNA expression profiling starts with extraction of total RNA from FFPE tissues. The purification process is critical for the performance of the analysis, and to assure reliable results of miRNA profiling the integrity of recovered RNA is assessed for quantity and quality [77]. In comparison studies dual-color staining is carried out, in which the respective physiological states are labelled with specific fluorescent dyes [77, 78]. The specimens are mixed pair-wise and sample RNAs are allowed to hybridize to complementary oligonucleotide capture probes attached to a solid support (Figure 10). The capture probes represent those miRNAs (for example, all known human miRNAs) intended to be investigated. Following hybridization, the array slide is scanned and the data are processed. By statistical analysis aberrantly expressed miRNAs could be identified and those with significant deregulation can be pointed out [79].

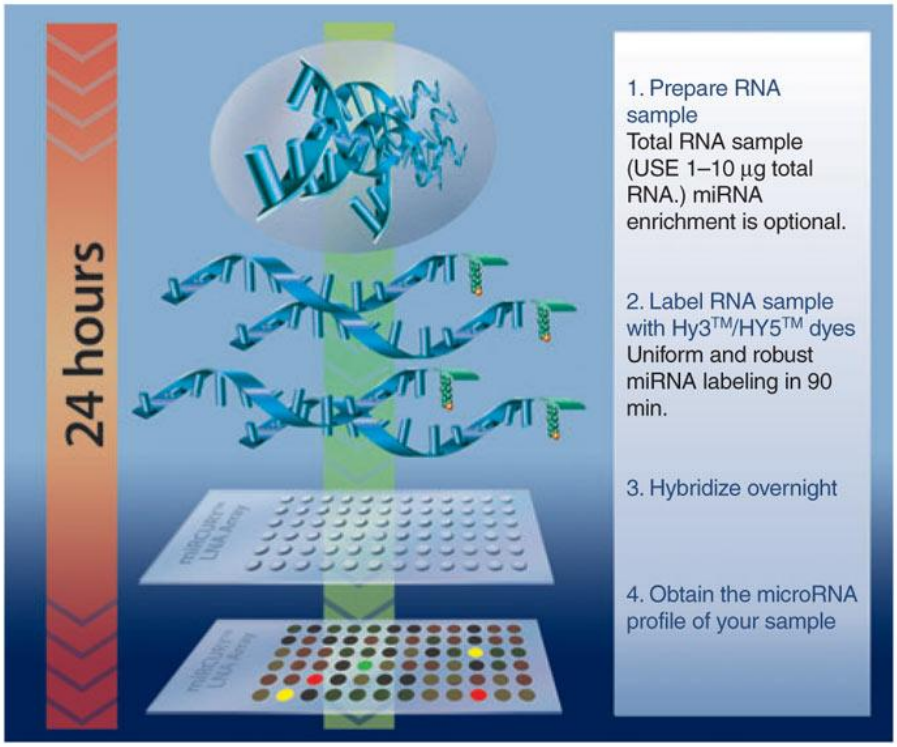

Figure 10. Basic steps in miRNA expression profiling [80]. Total-RNA recovered from the specimens is assessed for quantity and quality prior the experiment. The samples representing pathological and normal states are labelled with Hy3 green fluorescent dye and Hy5 red fluorescent dye, respectively, and then mixed pair-wise. Following the labelling reaction, the RNA samples are applied to the microarray slide containing LNA capture probes. The specimens are hybridized overnight, and then scanned. The generated expression data are processed to provide expression profiles showing the real biological impact of miRNA in the specimens. Statistical methods are used to recognize significantly differentially expressed miRNAs [80].

1.7.2 Technical aspects of microarray-based miRNA expression profiling

Expression profiling of miRNAs is more challenging than for DNA molecules due to the fact that miRNA molecules are characterized with short length and sequence similarity of closely related sequences. Additionally, this group of RNA is present in small amount, only 0.01% of total-RNA is represented by miRNA. The miRNA strands also have variable GC content meaning that the melting temperature (T_m) vary greatly among individual miRNAs [77]. These factors make it challenging to design capture probes exhibiting high affinity to target miRNAs. To tackle these problems different strategies have been tried, and the most successful was developed by the research group of Jesper Wengel in Denmark [81]. In 1998 they implemented detection probes based on locked nucleic acid (LNA) technology. LNA is a modified DNA monomer, in which the ribose ring is locked by a methylen bridge linking the 2'O atom and the 4'C atom, in order to form a nucleoside optimal for Watson-Crick base-pairing (Figure 11). Incorporation of LNA monomers into DNA probes enhance the melting

temperature (T_m) and allow base-pairing with high sensitivity and specificity to small RNA sequences, resulting in formation of stable miRNA duplexes [82].

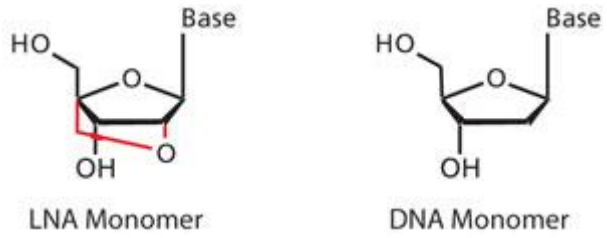

Figure 11. LNA monomer versus DNA monomer. In the LNA monomer a synthetic methylen-brige connects the 2' O atom and 4'C atom, in order to form a nucleoside ideal for Watson-Crick binding [83].

miRNA profiling are comprehensive experiments producing a massive amount of data. Often the generated data is influenced by factors that may cause systematic errors. Biased signal intensities across the microarray are frequent and can be explained by miRNA recovering, fluorescence labeling, and by the hybridization capacity. These factors are usually removed in a normalization process. In a filtering step the dimensionality of the raw expression data is reduced through elimination of miRNA-genes not differentiated enough [84, 85]. Spike-in controls containing non-human RNA transcripts are added to a number of capture probes, in order to reduce sample variations and to assess the real biological impact of miRNAs in the samples [78, 86].

1.7.3 Statistical methods for miRNA expression profiling

miRNA profiling was aimed to show possible trends of differentially expressed miRNAs for long DSS versus C, short DSS versus C, and long DSS versus short DSS. A number of statistical approaches were used to identify significant deregulated miRNAs. These include heat map and unsupervised hierarchical clustering, in which the relative miRNA expression was displayed graphically, and samples and miRNAs were clustered based on overall similarities in miRNA expression. Two-tailed t-test was used to prove whether it is significant differentiation in miRNA expression among the investigated groups [79]. Significant differentiated miRNAs with low p-value and +/- fold change more than two was easily identified in volcano plot.

1.8 miRNA *in situ* hybridization (miRNA ISH)

In situ hybridization (ISH) is a powerful method to investigate the biological role of DNA and RNA fragments in cells of different origin. The basic principle is simple Watson-Crick base-pairing between labelled nucleic acid probes and genetic material at precise locations in the cells [87]. In this way, the expression of biomarkers could be studied at cellular level under a microscope.

In recent time miRNA ISH has become an accurate tool in revealing the behavior of miRNAs in several diseases, and especially in cancers [88]. Concerning the protocol, miRNA ISH detection differ to some extent from conventional ISH protocols for DNA or RNA. Firstly, a hybridization buffer not containing the toxic agent formamide is used, which is found to detect miRNAs at high signal-to-noise ratio. Moreover, the acetylation step intended for reducing unspecific binding of the probe to amino groups and the and the post-fixation step used for preserving tissue and molecular target following proteolytic over-digestion are both omitted. To compenstate for these steps the proteinase-K treatment has been optimized to the highest level [89, 90]. As in the case of miRNA expression profiling, LNA probes are considered to have the best binding characteristics for ISH detection of miRNAs [88, 91]. Research groups in Denmark have developed a robust miRNA ISH protocol using LNA detection probes (Exiqon, Denmark) [90, 92]. In the procedure miRNAs become available through proteinase K treatment. Then, double digoxigenin (DIG) labelled LNA probes can hybridize to complementary miRNA sequences in the tissue. Alkaline phosphatase (AP) conjugated to the probes catalyzes the transformation of the substrates 4-nitro-blue tetrazolium (NBT) and 5-bromo-4-chloro-3'-indolylphosphate (BCIP) into a blue precipitate (Figure 12) [92].

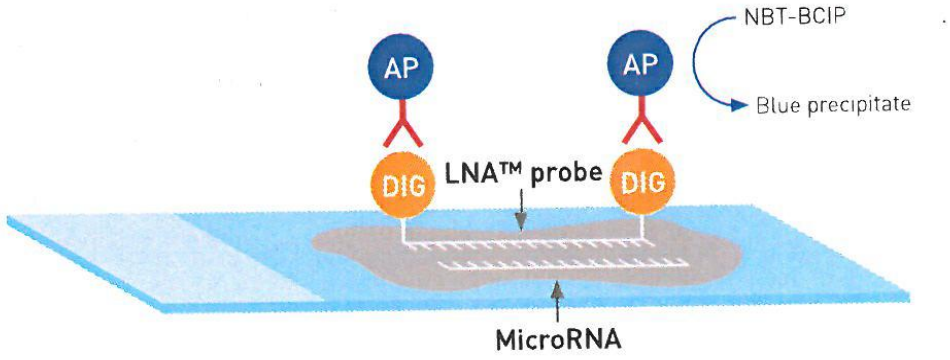

Figure 12. The principle of miRNA ISH detection. Double-digoxigenin (DIG)-labeled LNA™ (Exiqon) probes hybridize to targeting miRNA sequence. The digoxigenins then bound to specific anti-DIG, conjugated to alkaline phosphatise (AP). AP catalyzes the transformation of the substrates 4-nitro-blue tetrazolium (NBT) and 5-bromo-4-chloro-3'-indolylphosphate (BCIP) into a blue precipitate [92].

Aims of the thesis

- Establish Tissue Micro Array (TMA) cohorts of primary non-GIST soft tissue sarcomas (non-GIST STSs)
- Identify prognostic miRNAs involved in pathogenesis of selected patient groups by microarray-based miRNA expression profiling
- Study specific miRNAs in TMA cohorts including non-GIST STS samples by use of ISH analysis

2 Material and methods

2.1 Patients and clinical samples

The study was a part of the sarcoma project at the Norwegian Translational Cancer Research Center (NOTCH), UiT (University in Tromsø) The Arctic University of Norway. The research group was established in 2004 under the name of Translational Cancer Research Group by professor Roy Bremnes and professor Lill-Tove Busund. The group's research is based on studying molecular markers important for development of tumors in lung, connective tissues (sarcoma), prostate, and breast. By looking at the correlation between presence of interesting molecules and clinical data, it can provide information about diagnosis, prognosis, and response to cancer treatment. The fundamental strategy for the research involves construction of TMAs from archived biopsies that can be applied to downstream applications, such as IHC and ISH.

The sarcoma material included in the study consists of primary tumor tissue from anonymous patients diagnosed with sarcoma at the University Hospital in Northern Norway (UNN) and the Hospitals of Arkhangelsk County, Russia. The use of the archived patient material for research has been approved by National Cancer Data Inspection Board and the Regional Committee for Research Ethics [93]

In the database at UNN there were 632 registered patients during the period 1973-2006, and in Arkhangelsk 337 patients from 1994 to 2004 were registered (Figure 13) [94]. The shorter time period in Russia is due to less organized archive system during the Soviet regime. The obtained FFPE biopsies were re-evaluated according to current classification by two experienced pathologists. The tumors were graded in accordance with the French Fédération Nationales des Centre de Lutte Contre le Cancer (FNCLCC) and histologically subtyped

according to WHO classification system [94]. To be adaptable for the study the Russian biopsies were re-embedded at UNN and new H&E slides were made. For the Norwegian material new H&E slides were made when necessary. IHC staining with cytokeratin (CK, epithelial cell marker), CD117, actin and vimentin (markers for connective tissue), smooth muscle actin (SMA), and CD34 (endothelial cell marker) was performed on all biopsies, and S100 (malignant melanoma marker) to exclude differential diagnosis. Of the initial diagnosis 10 % were revised due to changes of the classification system and introduction of new subtypes, as for example gastro-intestinal stromal tumor (GIST). When excluding non-sarcomas, sarcomas not classified as STS, and GIST, the total number of non-GIST STS patients was 496. But of these, 247 patients were excluded because of insufficient clinical data (n=86) and inappropriate material (n=161) for histology. Then finally, 249 patients with non-GIST STS were qualified to be included in the NOTCH sarcoma project (UNN, n=167; Arkhangelsk n=82) [94].

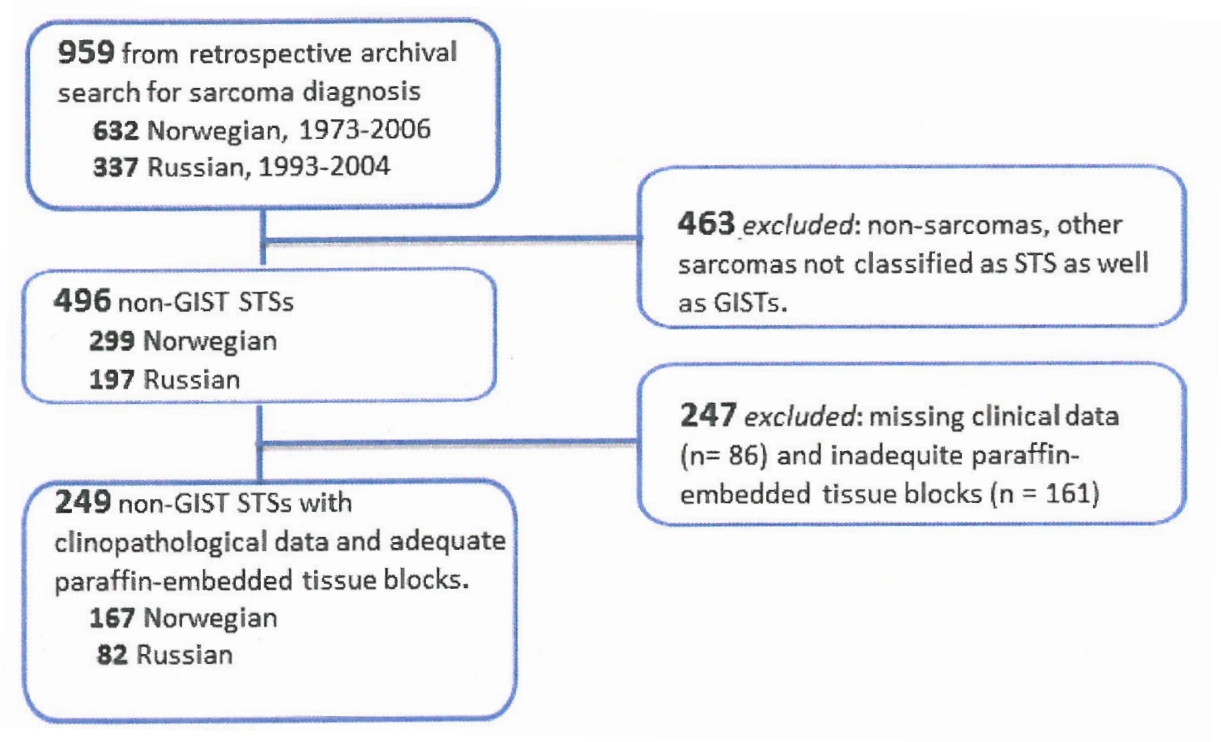

Figure 13. Flow-chart showing the exclusion and inclusion of samples in the NOTCH sarcoma project [94].

2.2 TMA construction

TMA cohorts were established for the 249 non-GIST STS cases. From each specimen tumor and stromal tissue cores were sampled to be distributed on different TMA blocks based on geographic location and type of tissue (Table 3).

Table 3. The arrangemant of TMAs.

Location	Type of tissue	Number of TMA blocks
UNN	Tumor	8
UNN	Stroma	2
Hospitals in Arkhangelsk County	Tumor	4
Hospitals in Arkhangelsk County	Stroma	1
		Total number: 15

Equipment for TMA construction

Product	Supplier
Recipient blocks (empty paraffin blocks)	Home- made
Microtome (Microm HM 355S)	Microm
Manual Tissue Arrayer (MTA-1)	Beecher Instruments
Punch needles 0.6mm	Estigen
Spreadsheet	
SuperFrost Plus glass slides	Thermo Scientific
Heat oven	Termaks

2.2.1 TMA procedure [70]

1. Biopsies and corresponding H&E slides were retrieved from histological archives.
2. Representative tumor and stromal areas were pre-marked on H&E slides by a pathologist. Red color was used for tumor tissue and green color for stromal tissue.
3. The design of TMA cohorts was decided. Initially, two cores of 1mm were punched, but during construction it was changed to four cores of 0.6mm to better preserve the donor blocks. It was planned to produce four TMA parallels to get more sample material for downstream analysis.
4. The recipient block was made by filling a large-sized metal mold with melting paraffin. A plastic cassette was attached on top of it and the construction was placed on a cooling plate for 10 min to harden the paraffin.
5. The metal mold was gently removed, and thus, the recipient block was made.
6. The recipient block was trimmed down to obtain a flat surface by using microtome (Microm HM355).

7. Before starting the TMA construction itself the biopsies and the H&E slides for each sample were organized in orderly rows on trays.
8. For each TMA cohort it was decided to construct four parallel blocks. The blocks were fastened in the four positions in the RBI-1 of the MTA-1.
9. The punching needles were navigated to the starting position in the lower left corner of the recipient block. The distance to the edges should be at least 4mm to prevent cracking of the block when punching.
10. The needles were checked for being perfectly aligned in the recipient block.
11. The TMA construction was started by punching a hole in the recipient block using the smaller recipient needle.
12. From a pre-marked area in the donor block, a tissue core was extracted using the larger donor needle, and then the core was gently pushed down in the pre-made hole in the recipient block. Repeat the step for the rest of the three TMA parallels.
13. The ID number for the biopsy in that position was noted in a spreadsheet.
14. The punching needles were moved 1mm horizontally to the next X-Y position using the micrometers. Step 11-14 was repeated until the microarray construction was completed. Asymmetric array patterns were produced to avoid confusing when orienting the TMA blocks in subsequent steps.
15. The ID position for each TMA spot noted on the spreadsheet was saved in an excel file.
16. The newly produced TMA blocks were placed in heat cabinet at 37º C for approximately 10 min to homogenize the tissue cores with the surrounding paraffin.
17. TMA sections of 4μm were cut and mounted on SuperFrost Plus glass slides using Micorom HM355. To save the TMA blocks 50 sections were cut at a time.
18. The sections were allowed to dry for a couple of hours in RT, and then placed in heat cabinet at 59º C for 4 hours.
19. The sections were taken out from the heat cabinet and dipped in melting paraffin, and then laid down on a slide tray for 15 min in room temperature to allow the paraffin to harden.
20. The TMA sections embedded in paraffin were organized in slide boxes and placed in cool room until analyzing.

2.3 miRNA screening

The intention of miRNA screening was to study global miRNA expression in human sarcomas. Two prognostic groups of the non-GIST-STS population were chosen to be included in the screening. The selection criteria used was time of disease-specific survival (DSS), of which the first group involved 11 patients of long DSS and the second group 10 patients of short DSS (Table 4). The specimens mainly represented two histological STS subgroups, LMS and MFH (Table 4). In addition, single cases of spindle cell sarcoma (SCS), malignant mesothelioma (MM), and dermatofibrosarcoma (DFS) were included. As control material 10 samples of benign connective tissue derived from skin and uterus were used. Tumor areas were identified and pre-marked on the corresponding H&E slides. From each specimen, minute amounts of tumor material were punched (using MTA-1) from which total-RNA was recovered. The screening was carried out through microarray-based expression profiling of all registered human, mouse, and rat miRNAs. The miRNA profiling itself and the data processing were outsourced to Exiqon, Denmark.

Table 4. The samples included in miRNA screening

Sample number	Diagnosis	Prognostic group	Survival time (month)
S1	MFH	Short DSS	2
S2	MFH	Short DSS	10
S3	MFH	Short DSS	13
S4	SCS	Short DSS	13
S5	MM	Short DSS	16
S6	LMS	Short DSS	28
S7	LMS	Short DSS	29
S8	MFH	Short DSS	29
S9	LMS	Short DSS	38
S10	xx	Short DSS	xx
S11	LMS	Long DSS	41
S12	MFH	Long DSS	158
S13	MFH	Long DSS	170
S14	MFH	Long DSS	203
S15	LMS	Long DSS	219
S16	LMS	Long DSS	235
S17	MFH	Long DSS	287
S18	LMS	Long DSS	309
S19	DFS	Long DSS	313
S20	LMS	Long DSS	329
S21	LMS	Long DSS	207
S22	Benign	Control/uterus	
S23	Benign	Control/ mucosa	
S24	Benign	Control/uterus	
S25	Benign	Control/uterus	
S26	Benign	Control/uterus	
S27	Benign	Control/skin	
S28	Benign	Control/skin	
S29	Benign	Control/skin	
S30	Benign	Control/skin	
S31	Benign	Control/skin	

*incorrect labelling of sample, thus no clinical data available

2.3.1 Total-RNA isolation

Total-RNA from tumor areas of the selected samples was extracted using RecoverAll™ Total Nucleic Acid Isolation Kit for FFPE (Ambion) [95]. Equipment and material needed for the performance of RNA recovery are listed below.

Kit	Supplier
RecoverAll™ Total Nucleic Acid Isolation Kit for FFPE	Ambion life technologies

Material included in the kit

Product	Amount	Storage
Digestion buffer	16mL	Room temp (RT)
Wash 1 concentrate: Add 42 mL 100% ethanol before use	60mL	RT
Wash 2/3 concentrate: Add 48 ml 100% ethanol before use	60mL	RT
Collection tubes	80	RT
Filter cartridges	40	RT
Isolation additive	19.2mL	RT
Elution solution	5 mL	Any temperature
Protease	160µL	-20º C
10x DNase buffer	240µL	-20º C
DNase	160µL	-20º C
RNase A	400µL	-20º C

Material not included in the kit

Product	Supplier
Manual Tissue Arrayer (MTA-1)	Beecher Instruments
Punch needles 0.6mm	Estigen
Eppendorf tubes 1.5mL (there is no requirement for nuclease-free tubes)	Sarstedt
RNase Decontamination solution, RNase *Zap*	Ambion
Xylene	Fluka Analytical
Ethanol absolute	Sigma Aldrich
Adjustable pipettes	Biohit
RNase free tips	Art Molecular BioProducts
Microcentrifuge (Heraeus Biofuge Pico)	DJB labcare
Vortex (Reax top)	Heidolph
Heat block	Grant QBT2

Total RNA isolation procedure

Precautions

To maintain RNAse free environment the lab bench, pipettes, and sampling equipment must be cleaned with RNase*Zap* solution. Lab coats and disposable gloves should be worn at all times. Gloves prevent nucleic acids and RNases on the skin from contaminating sample RNA, and additionally, they protect the skin from reagents [95].

Sampling of tumor material

1. Tumor areas of the biopsies were pre-marked on corresponding H&E slide by a pathologist.

2. Sample material was obtained through punching 3x tissue cores of 0.6mm (approximately 35mg) using MTA-1.
3. The cores were collected in 1.5mL eppendorf tube, labeled with the associated biopsy number.

Between each sample all contact surfaces were cleaned with RNase*Zap*.

Total-RNA isolation (RecoverAll Total Nucleic Acid Isolation Protocol, Ambion) [95]

Deparaffinization

1. 1mL 100% xylene was added to eppendorf tube containing sample cores.
2. The tubes were mixed by a short vortex.
3. The samples were centrifuged briefly to obtain all tissue in the xylene in the bottom of the tube.
4. The samples were heated in 50º C for about 8 min to melt the paraffin.
5. The samples were centrifuged for 2 min at RT and 13 000x g to form a pellet.
6. Without touching the pellet the xylene was gently removed and eliminated.
7. 1mL of 100% ethanol was added to the sample. By a brief vortex mix the samples became opaque.
8. The samples were centrifuged for 2 min at RT and 13 000x g to form a pellet.
9. Without touching the pellet the ethanol was gently eliminated. The ethanol contains minute amounts of xylene that was discarded by repeating step 8-10 for 5-7 times.
10. The remaining drops of ethanol were collected by a brief centrifugation. The pellet was allowed to dry for 15-45 min at RT.

Protease treatment

11. To each sample 200µL of Digestion buffer and 4µL of protease was added. The tubes were swirled gently to mix the tissue contents with the solution. The tubes were centrifuged if necessary.
12. The samples were incubated for 15 min at 50º C and then 15 min at 80º C.

RNA-isolation

13. 240µl Isolation additive and 550µL 100% ethanol was added to each of the samples.
14. The samples were mixed by pipetting up and down to turn white and cloudy.
15. A filter cartridge was placed on a collection tube, and 700µL of the sample/ethanol solution was pipetted onto that filter cartridge, and the lid was closed.
16. The samples were centrifuged at 10 000 rpm for 30 sec to allow the mixture to pass through the filter.

17. The collection tube was emptied, and the centrifugation was repeated until all the solution has been passed through the filter.
18. 500µL of Wash 2/3 was added to the filter cartridge.
19. The samples were centrifuged at 10 000 rpm for 30 sec to allow the mixture to pass through the filter.
20. The collection tube was emptied, and the filter cartridge was re-inserted into the same collection tube.
21. The samples were centrifuged for 30 sec to discard fluid residues from the filter.

DNase treatment and final nucleic acid purification

22. The DNase mix was made.

Volume (µL per reaction)	Component
6	10X DNase buffer
4	DNase
50	Nuclease-free water

23. 60µL of the DNase mix was added to the centre of the filter cartridge.
24. The lid was put on the tube and incubated for 30 min at RT.
25. 700µL of Wash 1 was added to the filter cartridge.
26. The samples were incubated for 30-60 sec at RT.
27. The samples were centrifuged for 30 sec at 10 000 rpm.
28. The collection tube was emptied, and the filter cartridge was re-inserted to the same collection tube.
29. 500µL of Wash 2/3 was added to the filter cartridge.
30. The samples were centrifuged for 30 sec at 10 000 rpm.
31. The collection tube was emptied, and the filter cartridge was re-inserted to the same the same collection tube.
32. Step 30-31 were repeated for a second wash of 500µL of Wash 2/3.
33. The samples were centrifuged for 1 min at 10 000 rpm to remove fluid residues from the filter.
34. The filter cartridge was placed into a fresh collection tube.
35. 60µL of Elution solution was added to the centre of the filter, and the lid was closed.
36. The samples were incubated for 1 min at RT.
37. The samples were centrifuged for 1 min at 13 000 rpm to allow the mixture to pass through the filter. The eluate contains recovered RNA.

Assessment of quantity and quality of isolated total-RNA

Isolated RNA from the samples was subject for quantity and quality assessment on NanoDrop Spectrophotometer (ND 1000) [96]. Nucleic acid concentration was determined by measuring the absorption of UV light at 260nm. By applying Beer-Lambert law the amount of absorbed UV correlate to the concentration of nucleic acid. The purity of nucleic acids is assessed in relation to proteins and organic compounds. The ratio 260/280 is used to determine the degree of protein contamination (280nm = peak absorbance for proteins), whereas the ratio 260/230 is used to determine the degree of contamination of organic compounds (230nm = peak absorbance for organic compounds). For pure RNA the ratio should be around 2 for both 260/280 and 260/230. Values lower than that indicates contamination.

2.3.2 Global microarray-based miRNA expression profiling

miRNA expression profiling was outsourced to Exiqon. In the attachment "MicroRNA Array Final Services Report", the procedure are described [79].

The total number of samples was 31; 11 cases with long DSS, 10 cases with short DSS, and 10 C samples. Recovered miRNA from the samples were fluorescence labeled with Hy3™ and the reference pool containing a mix of small amounts from all samples was fluorescence labeled with Hy5™. Spike-in controls of different concentrations were added to the specimens to compensate for sample variances. Global profiling was carried out on all human, mouse, and rat miRNAs verified in miRBase (n=1274). The fluorescence signals were normalized by use of a mathematical regression algorithm.

Statistical analysis of miRNA expression profiling

The raw array data was processed by Exiqon and sent electronically to the writer. The expression data for all the samples were saved in an excel file (41 014 kB) and in the "MicroRNA Array Final Services Report" the main results were summarized. At UiT the data was evaluated. Statistical approaches including; heat map and unsupervised hierarchical clustering, and volcano plots, were used to identify aberrantly expressed miRNAs [79].

2.4 miR-126 *in situ* hybridization (miR-126 ISH)

miR-126 ISH was performed on the whole non-GIST STS material (n=249). miRCURYLNA™ microRNA ISH Optimization Kit (FFPE) (Exiqon, Denmark) was

employed in the study [92]. The protocol, "One-day microRNA ISH protocol", was modified to some extent at UiT to be adaptable for the TMAs produced for the NOTCH projects.

2.4.1 Equipment used for miR-126 ISH [92]

Kit	Supplier
miRCURYLNA™ microRNA ISH Optimization Kit (FFPE)	Exiqon, Denmark

Reagents included in the kit

Product	Amount	Conc.	RNA T_m
Double-DIG labeled Detection probe: hsa-miR-126 (Exiqon, Product No. 88067-15),	40µL	25µM	84°C
microRNA ISH (hybridization) buffer (2x)	25mL		
Proteinase-K, lyophilized	12mg		

Controls [92]

Product	Amount	Conc.	RNA T_m
Positive control: LNA™ U6 snRNA probe, (5'-cacgaatttgcgtgtcatcctt-3')	40µL	0.5µM	84°C
Negative control: LNA™ scrambled miRNA probe (5'-tgtaacacgtctatacgccca-3')	40µL	25µM	87°C

The positive U6 probe contains a non-coding RNA transcript detected in the nucleus in all cells [89]. The negative scramble probe contains a genetic sequence with no complementarity to any miRNA sequences in human, mouse and rat [90]. A TMA block containing a range of different malignancies was used as control material.

Reagents not included in the kit

Reagent	Supplier
Xylene	Fluka Analytical
Ethanol absolute	Sigma Aldrich
Diethyl pyrocarbonate (DEPC)	Sigma Life Sciences
Proteinase K buffer:	
1M Tris-HCl pH 7.5	Invitrogen
0.5M EDTA	Appliled biosystems
5M NaCl	Ambion
RNase free water (DEPC water)	Prepared in-house
20x stringency washing (SSC)	VWR
PBS tablets	Sigma Aldrich
Tween 20	Sigma Aldrich
Normal Sheep Serum	Jackson ImmunoReseach

continuation

DIG Wash and Block Buffer Set including 10x Maleric acid and 10x Blocking solution	Roche
NBT/BCIP ready-to-use tablets	Roche
anti-DIG-AP Fab fragments	Roche
Levamisole	Sigma Aldrich
KTBT buffer:	
50mM Tris-HCl	Sigma Aldrich
150mM NaCl	Sigma Aldrich
10mM KCl	Sigma Aldrich
Nuclear Fast Red	Chroma

Materials not included in the kit

Product	**Supplier**
Latex gloves	OneMed
Heat oven	Termaks
Slide frame	
Bench coat	
Waste box	Cerbo
Choplin jars	
Dako Pen	DAKO
Heat block	Grant QBT2
Sterile glass pipettes	Falcon
Adjustable pipettes	Biohit
Sterile filter tips	ART Molecular BioProducts
Glass bottles 1L	VWR
Centrifuge tubes 50mL	VWR
Cell culture bottles 160mL	Nunc
Microcentrifuge	VWR
Hybridization station	VYSUS HYBrite
Hybridization cover; HybriSlip™	Sigma Aldrich
Syringes	BD
Pipetboy	Integra Biosciences
Fixogum	Marabu
Mounting medium (Histokit)	VWR
Coverslips	Menzel Gläser
Microscope	Leica
Surgical blades	Swann Morton

2.4.2 Preparation of reagents [97]

0.1% DEPC water

Components	Concentration	Volume	Storage temp
Diethylpyrocarbonate (DEPC)	0.1%	1mL	4-8ºC
milliQ water		1L	

Preparation of DEPC was performed in fume hood since it is toxic and carcongenic.
The solution was incubated overnight at 37º C, and autoclaved. Ready-to-use DEPC water was stored at 4-8º C.

PBS buffer

Components	Concentration	Amount	Storage (temp)
PBS tablets		5 tablets	RT
DEPC water	0.1%	1000mL	4-8º C
		Autoclavation	4-8º C

PBS-T buffer

Components	Concentration	Amount	Storage (temp)
PBS pH 7.2-7.6		300mL	4-8º C
Tween 20		300µL	RT

Proteinase K treatment

Tris-HCl, 10mM

Components	Concentration	Volume	Storage (temp)
1M Tris-HCl pH 7.5	10mM	10µL	RT
DEPC water	0.1%	990µL	4-8º C

Proteinase K stock, 20 mg/mL

Components	Amount	Volume	Storage (temp)
Proteinase K (lyophilized)	12 mg		-20º C
Tris-HCl pH 7.5	10mM	600µL	RT

Proteinase K was properly solved and aliquots of 10µL was distributed in RNase free tubes and stored at -20º C

Proteinase K buffer

Components	Concentration	Volume	Storage (temp)
Tris-HCl pH 7.5	1M	5mL	RT
EDTA	0.5M	2mL	RT
NaCl	5M	2mL	RT
DEPC water	0.1%	Adjust to 1000mL	4-8º C
		Autoclavation	4-8º C

Proteinase K reagent, 1:1000

Components	Concentration	Volume	Storage (temp)
Proteinase K stock	20 mg/mL	10µL	-20º C
Proteinase K buffer		10mL	4-8º C

Proteinase K was prepared prior to use.

Hybridization

Hybridization mix buffer, 1:1

Components	Concentration	Volume	Storage (temp)
ISH buffer		500µL	4-8º C
DEPC water		500µL	4-8º C

The hybridization mix was prepared prior to use.

U6 snRNA probe, 50nM

Components	Concentration	Volume	Storage (temp)
U6 snRNA probe	0.5µM	2µL	-20º C
Hybridization mix buffer	1:1	1000µL	4-8º C
			-20º C

Scramble miRNA probe, 50nM

Components	Concentration	Volume	Storage (temp)
Scramble miRNA probe	25µM	2µL	-20º C
Hybridization mix buffer	1:1	1000µL	4-8º C
			-20º C

hsa-miR-126 probe, 25nM

Components	Concentration	Volume	Storage (temp)
hsa-miR-126 probe	25µM	1µL	-20º C
Hybridization mix buffer	1:1	1000µL	4-8º C
			-20º C

Stringency washing

5x SSC

Components	Concentration	Amount	Storage (temp)
SSC	20x	10mL	4-8º C
DEPC water	0.1%	990mL	4-8º C
		Autoclavation	4-8º C

1x SSC

Components	Concentration	Amount	Storage (temp)
SSC	20x	10mL	4-8º C
DEPC water	0.1%	990mL	4-8º C
		Autoclavation	4-8º C

0.2x SSC

Components	Concentration	Amount	Storage (temp)
SSC	20x	10mL	4-8º C
DEPC water	0.1%	990mL	4-8º C
		Autoclavation	4-8º C

Blocking

1x Maleric acid

Reagent	Concentration	Amount	Storage temp
Maleric acid retrieved from DIG Wash and Block Buffer Set	10x	2mL	RT
DEPC water	0.1%	18mL	4-8º C/RT

Maleric acid was prepared prior to use.

Sheep serum

Components	Concentration	Amount	Storage temp
Sheep serum (lyophilized)	60 mg/mL		-20º C
DEPC water	0.1%	10mL	4-8º C/RT

Aliquots of 250µL were prepared and stored at -20º C.

1x Blocking solution

Reagent	Concentration	Amount	Storage (temp)
Blocking solution retrieved from DIG Wash and Block Buffer Set	10x	2mL	-20º C
Maleric acid	1x	17.6mL	RT
Sheep serum		400µL	-20º C

The blocking solution was prepared prior to use.

Anti-DIG AP reaction

Anti-DIG AP

Reagent	Concentration	Amount	Storage (temp)
Blocking solution	1x	8mL	
Anti-DIG-AP		10µL	4-8º C/RT

Anti-DIG AP was prepared prior to use

AP substrate reaction

Levamisole, 100mM stock

Components	Concentration	Amount	Storage (temp)
Levamisole	240.75 g/mol	250mg	
DEPC water	0.1%	10.4mL	4-8º C

Levamisole was dissolved in DEPC water, and the solution was transferred to a cell culture bottle.

AP substrate

Reagent	Concentration	Amount	Storage (temp)
NBT/BCIP tablets		1 tablet	4-8º C
DEPC water	0.1%	10mL	4-8º C
Levamisole	100mM	20µL	

AP substrate was prepared prior to use.

Stopping the AP substrate reaction

KTBT buffer

Components	Concentration	Amount	Storage (temp)
Tris-HCl	50mM	7.9g	RT
NaCl	150mM	8.7g	RT
KCl	10mM	0.75g	RT
DEPC water	0.1%	Adjust to 1000mL	4-8º C

2.4.3 miR-126 ISH assay

miR-126 ISH analyzing is an extensive experiment involving a lot of hands-on work (Table 5). During the whole process, it was important to maintain RNase free environment to prevent contamination of sample RNAs [90]. All equipment should be sterile or autoclaved, and it is recommended to wear lab coat and disposable gloves. The lab work must be done with care and accuracy. For example, ensure correct pipetting and prevent the tips from being in contact with other objects.

Table 5. Outline of the miRNA ISH protocol [92]

Step	Process	Time (min)
1	Deparaffinization	40
2	PBS wash	5
3	Proteinase-K treatment	20
4	PBS wash	5
5	Dehydration	20
6	*In situ* hybridization	60
7	Stringent washes (SSC)	30
8	PBS wash	5
9	Blocking	15
10	Anti-DIG-AP	30
11	PBS-T (0.1% Tween 20) wash	10
12	AP reaction	90
13	Stop AP reaction (KBTB buffer)	10
14	Counter staining	10
15	Dehydration	10
16	Mounting	5
	Total time: approximately 7 hours	

Optimization of protocol

Before starting miR-126 ISH analysis on the sample material it was necessary to optimize the protocol in order to obtain clear and specific staining. Critical parameters for the staining results cover the proteinase-K treatment, titer of the detection probe, and hybridization

temperature [89]. The proteinase-K step highly depends on the fixation conditions of the tissue, and considering the hybridization temperature, it should be highest possible to avoid cross-binding of similar complementary sequences [90].

When optimizing the protocol, the positive U6 control, the negative scramble control, a tissue slide known to be positive for miR-126, and a TMA slide from the study were included. Concentrations of 25nM, 50nM, and 100nM of miR-126 detection probe were tested at hybridization temperature 50º C. In collaboration with pathologist Lill-Tove Busund the staining results were evaluated, and we decided that the concentration of 25nM should be used. The concentrations of 50nM and 100nM showed a tendency of overstaining.

2.4.4 miR-126 ISH protocol

(Based on Exiqon's "One-day microRNA ISH protocol") [97]

The samples distributed on 15 TMA sections must be analyzed in two runs because of limited capacity of the hybridization station (10 positions). In each run, positive (U6) and negative (scramble) controls were included.

Deparaffinization

1. The day before, the slides were set horizontally in stand, and placed in heat oven at 59º C to melt the paraffin.
2. The sections were deparaffinised through a series of xylene and ethanol bathes. Choplin jars were used, and it was performed in laminar hood.

Reagent	Time (min)
Xylene	5
Xylene	5
Xylene	5
Absolute ethanol	5
96% ethanol	5
70% ethanol	5
PBS	2-5

3. To achieve equal reaction conditions for all tissue cores on the TMAs, a hydrophobic barrier was created around the array area using a Dako Pen.

Proteinase K treatment

4. Proteinase K reagent was prepared (see the preparation protocol above).
5. The sections were laid horizontally on a slide rack and 1000µL proteinase K was added to each TMA section.

6. The slides were incubated for 20 min at 37º C using VYSIS HYBrite.
7. 2x PBS wash
8. Dehydration

Reagent	Time (min)
70% ethanol	1
96% ethanol	1
Absolute ethanol	1

9. The sections were air dried for 15 min on clean paper at RT.

Denaturing

10. Hybridization mix buffer was prepared (see preparation protocol down below).
11. Aliquot of miR-126 detection probe was taken from the freezer and thawed.
12. Appropriate volume required for the experiment was pipetted into a RNase free eppendorf tube, and then denatured for 4 min at 90º C using Grant QBT 2 heat block.
13. The volume was spun down and diluted with hybridization mix buffer to obtain the selected miR-126 probe concentration.
14. The sections were laid horizontally on a slide rack and 80µL of the miR-126 and control detection probes were applied to each of the slides.
15. The array area was covered with hybrislips to optimize the hybridization conditions. The hybrislips were sealed to the sections with Fixogum.
16. The TMA sections were hybridized in 60 min at 50º C in VYSIS HYBrite.
17. When hybridization was finished the hybrislips were carefully removed using surgical blade.

Stringency washing

18. The sections were passed through a series of SSC buffers.

Concentration	Time (min)	Temperature
5x SSC	5	RT
5x SSC	5	56º C
1x SSC	5	56º C
1x SSC	5	56º C
0.2x SSC	5	56º C
0.2x SSC	5	56º C
0.2x SSC	5	RT
PBS		RT

Blocking

19. The blocking solution was prepared (see preparation protocol above).
20. 800µL of the solution was added to each section.

21. The slides were incubated for 15 min in humidified chamber at RT.

Antibody reaction

22. Sheep anti-DIG-AP solution was prepared (see preparation protocol above).
23. 500µL of the solution was added to each slide.
24. The sections were incubated for 30 min at 30º C using VYSIS HYBrite.
25. 3x3 min PBS-T washing.

AP-substrate reaction

26. AP-substrate solution was prepared (see preparation protocol above).
27. 500µL of the solution was added to each section.
28. The sections were incubated for 90 min at 30º C using VYSIS HYBrite.
29. The substrate reaction was stopped through passing the sections 2x 5 min in KTBT buffer.
30. 2x1 min in tap water.

Counterstaining

31. The sections were dipped for one minute in Nuclear Fast Red.
32. The sections were rinsed thoroughly in tap water.

Dehydration

33. The sections were dehydrated according following procedure.

Reagent	**Number of dips**
70% ethanol	10
96% ethanol	10
96% ethanol	10
Abs ethanol	10
Abs ethanol	

Mounting

34. The sections were mounted using coverslips and Histokit.
35. The sections were dried overnight in laminar hood.
36. Following day the staining of the TMA sections were checked under microscope. The positive U6 snRNA control should have intense nuclear staining, and the negative scramble miRNA control should be clearly negative. Also verify that the staining of the TMA sections were adequate, and no tendency of uneven staining.

2.4.5 Practical aspects of miR-126 ISH

Several factors might affect the result of *in situ* detection of miRNAs. Pre-analytical variables, such as improper fixation of removed tissue or storage conditions of biopsies, could lead to miRNA degradation. Analytical factors, including RNase contamination, thickness of TMA sections, proteinase-K treatment, incorrect incubation temperatures, or inaccurate concentration of probes and reagents, may all influence the reliability of the staining results [90, 97]. In the present study, there were concerns regarding different fixation and storage conditions between the Norwegian and Russian material, not maintaining RNase free environment during TMA construction, and use of too thin TMA section (4µm instead of recommended 5-7µm). But, in evaluation of the miRNA ISH staining by the writer and Andrej Valkov it could not be demonstrated any significant impact of any of these factors. Notably, it is reported that miRNAs recovered from FFPE biopsies are more reliable as an analytic component than mRNAs, because their short length makes them more stable and better suited for long-time storage in histological archives [77]. In contrast, the longer mRNA sequences are more fragile and less credible in analysis of tissue material.

2.4.6 Scanning and scoring of miR-126 ISH-staining using Ariol imaging system

The expression of miR-126 in the tissue cores were scanned and digitized using Ariol imaging system (Genetix, San Jose, CA).

Ariol imaging system

Ariol imaging provides high-throughput scanning of IHC and ISH stained tissue sections. The system consists of the software package, a slide holder rooming 50 sections, a robotic arm, Olympus BX61 microscope, and a computer screen (Figure 14) [98]. Cell-type specific expression of biomarkers were digitized and shown on the computer screen. The high resolution of morphological details enables properly scoring of IHC or ISH stained molecular markers.

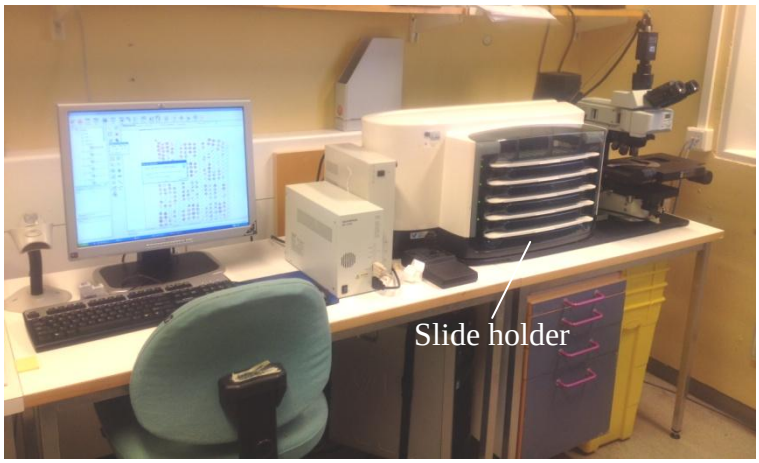

Figure 14. The Ariol imaging system provides digital imaging and scanning of IHC and ISH stained histological sections. The platform includes the software package, the computer screen, the slide holder, and the microscope [98]. The Ariol platform at IMB, UiT.

Scoring of miR-126 expression on Ariol imaging system

(The procedure for Ariol system used at UiT) [99]

1. The TMA slides were labelled with bar codes and placed on the Ariol slide holder.
2. The sections were pre-scanned at low resolution (1.25x objective).
3. The cores of the TMAs were arranged into a coordinate system.
4. Main scanning of the samples was performed at high resolution (20x objective). The time for main scanning for the TMAs included in the study was approximately two days.
5. The sample cores were sorted based on staining density.
6. The miR-126 expression for all array cores were displayed on the computer screen, and then scored manually by two independent observers using a semi quantitatively scale.

A semi quantitatively scale ranging from 0 to 4 was used to assess the degree of miR-126 staining. A zero (0) value indicates no staining; 1 weak staining; 2 moderate staining; 3 strong staining; and 4 inconclusive for being assessed. The reason for no scoring (4) could be due to a missing core, not enough material, or not representative material. The intensity of miR-126 expression was scored by the writer and pathologist Andrej Valkov independently of each other.

2.4.7 Statistical analysis of miR-126 ISH

The statistical software package SPSS version 19 (Statistical Product and Service Solutions, Chicago IL) was used to analyze the scoring results from miR-126 ISH. The scores from each observer were compared for interobserver reliability by use of a two-way random effect model with absolute agreement definition. The intraclass correlation coefficient (reliability coefficient) was obtained from these results. Plots of the DSS according to marker expression were drawn using the Kaplan-Meier (KM) method, and statistical significance between survival curves was assessed by the log rank test. DSS was determined from the date of surgery to the time of sarcoma death.

3 Results and discussion

3.1 Tissue Micro Array (TMA)

TMA cohorts containing primary tumors from sarcoma patients were produced as a part of the NOTCH sarcoma project at UiT. During construction of the TMA blocks there were some challenges due to the fact that sarcoma represents a heterogenous group of histological subtypes derived from a range of different tissues. For example tissues, such as skin and bone were tough to extract for the 0.6mm needles. The TMAs produced for the sarcoma project have successfully been used to study the correlation between molecular expression and clinical data in soft tissue sarcomas [93, 94].

3.2 Assessment of quantity and quality of total-RNA isolation

Total-RNA isolated from 31 samples was assessed both at UiT and Exiqon before the performance of microarray-based global miRNA expression profiling. The quantity and quality data of recovered RNA are shown in Table 6. The amount of recovered RNA were generally assessed to be higher at Exiqon, and also concerning the purity, the Exiqon data seemed to be more stable. The reason for some of the extreme values measured at UiT is not clear, but generally the amount of extracted RNA was low and close to the detection limit in the OD range of the Nanodrop instrument, resulting in reduced accuracy of RNA assessment. Nevertheless, Exiqon approved all samples for downstream miRNA expression profiling.

Table 6. Sample quality control of recovered total-RNA

Sample number	Prognostic group	Data supplied by UiT			Data supplied by Exiqon		
		Conc (ng/µL)	OD 260/280	OD 260/230	Conc (ng/µL)	OD 260/280	OD 260/230
S1	Long DSS	101	2.19	0.94	99	2.01	0.60
S2	Long DSS	83	1.53	1.16	84	1.89	0.79
S3	Long DSS	77	2.22	2.87	84	1.89	1.18
S4	Long DSS	31	2.65	-27.97	121	1.83	1.10
S5	Long DSS	46	2.21	5.12	48	1.94	1.27
S6	Long DSS	31	1.93	-6.55	58	1.73	1.12
S7	Long DSS	26	2.26	-8.44	51	1.82	1.03
S8	Long DSS	106	2.14	0.84	38	2.01	1.55
S9	Long DSS	45	2.24	1.03	119	1.92	0.64
S10	Long DSS	48	2.41	3.42	54	1.91	1.02
S11	Long DSS	36	2.44	-7.93	62	1.98	1.24
S12	Short DSS	22	2.39	0.97	48	1.76	0.49
S13	Short DSS	47	2.38	1.75	33	2.01	0.84
S14	Short DSS	13	3.00	0.44	57	1.83	0.30
S15	Short DSS	31	2.61	50.83	21	1.92	0.97
S16	Short DSS	-0.36	20.82	-0.06	46	1.39	0.14
S17	Short DSS	40	2.23	0.31	6	1.93	0.26
S18	Short DSS	17	0.86	-1.09	53	1.87	1.12
S19	Short DSS	57	2.00	2.16	27	1.91	1.15
S20	Short DSS	155	2.06	2.92	73	1.97	1.75
S21	Short DSS	74	2.22	2.14	167	1.94	1.12
S22	Control	67	2.39	0.67	93	2.01	0.53
S23	Control	27	2.35	12.54	89	1.94	1.05
S24	Control	33	2.34	1.54	41	1.93	0.73
S25	Control	44	2.29	3.14	46	1.97	1.11
S26	Control	77	2.20	0.66	54	2.07	0.50
S27	Control	39	2.50	1.19	88	1.97	0.63
S28	Control	17	2.41	0.16	52	1.62	0.20
S29	Control	33	2.53	-9.62	36	2.00	1.10
S30	Control	20	3.00	-25.65	44	2.06	0.87
S31	Control	30	2.46	-7.92	41	2.04	1.11

3.3 Microarray-based global miRNA expression profiling

The global miRNA expression profiling was outsourced to Exiqon and the results were returned electronically. A summary of the analyzing results is found in the attachment "MicroRNA Array Services Final Report". In the following sections, 5.3.1-5.4, the results of the miRNA profiling are shown and discussed.

3.3.1 Heat map and unsupervised hierarchical clustering

In the diagram the samples are displayed in columns and the miRNAs in rows, and the relative level of miRNA expression is illustrated by a color scale ranging from blue to red (Figure 15). The cluster trees on top and on the left side of the diagram represent overall similarities in miRNA expression for samples and miRNAs, respectively. Those 50 miRNAs with highest standard deviation (i.e. largest variation) were subjected for hierarchical clustering. The clustering on top shows the categorization of samples into two main groups, and then further division into smaller subgroups based on miRNA representation. The group on the left side mainly represent the MFH specimens and the group on the right side represent the LMS samples. However, two LMS cases were grouped together with the MFH cluster. Additionally, the two patients with SCS and the one with DMS were found in that group also. In spite of these conflicting results, it was a trend showing differential miRNA expression for LMS and MFH, meaning that the tumorigenesis for these sarcoma types involve specific subsets of miRNAs. Also the normal samples were differentially clustered, those found on the left end of the diagram derived from skin, and those located on the right part originate from uterus. Summarized, the hierarchical clustering of samples reflects their histological origin.

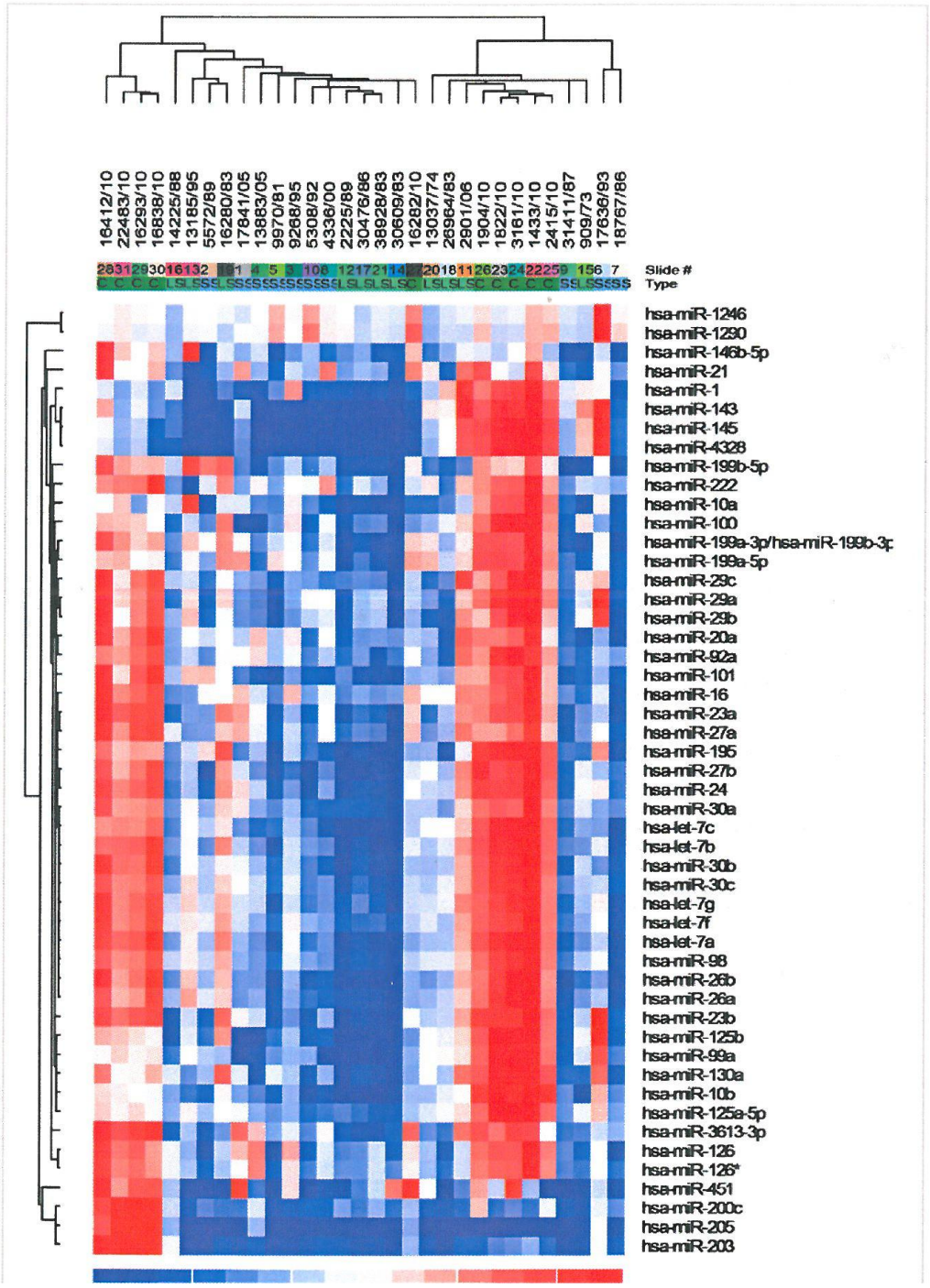

Figure 15. Heat map and unsupervised hierarchical clustering of sarcoma samples of long DSS (n=11) and short DSS (n=10), and Cs (n=10). Those 50 miRNAs with largest variation are included. The heat map illustrates the relative miRNA expression level in the samples using the color scale, ranging from blue to red. The cluster trees represent overall similarities in miRNA expression for samples and miRNAs, respectively. The blue columns indicate general downregulation of miRNAs in the sarcoma samples relative to Cs. The clustering tree on top divide the samples into two major groups, representing LMS (left part) and MFH (right part). Also the C samples were grouped in accordance with histological origin.

3.3.2 Differentially expressed miRNAs – short DSS versus control (C)

Two sample t-test was used to determine whether there are unequal variances for short DSS and C. Differentially expressed miRNAs could then be recognized in a volcano plot (Figure 16). The x-axis in the diagram describes the change between the two states (short DSS-C) using deltaLogMedianRatio (dLMR) (also referred to fold change), and the y-axis show the significance using –log10 p-value. Significant deregulated miRNAs were defined as dLMR > +/-1.0 (=fold change +/-2), 4.00 –log10 p-value ($p<0.001$), and displayed as red plots in the volcano plot. Negatively expressed miRNAs were shown in the left side of the x-axis and positively expressed in the right part, and with increasing significance toward the top. Non-significant miRNAs were marked as blue plots.

In the processing by Exiqon, 54 of 1274 miRNAs were defined as significant ($p< 0.000117$, dLMR > +/- 1.0), and most of them were downregulated. The 15 miRNAs exhibiting highest dysregulation are listed in Table 5. The negative values in the dLMR column highlight the general suppression of miRNAs in sarcoma.

Notably, the p-values operated by Exiqon are very low, higher p-values would generate a significantly greater amount of deregulated miRNAs.

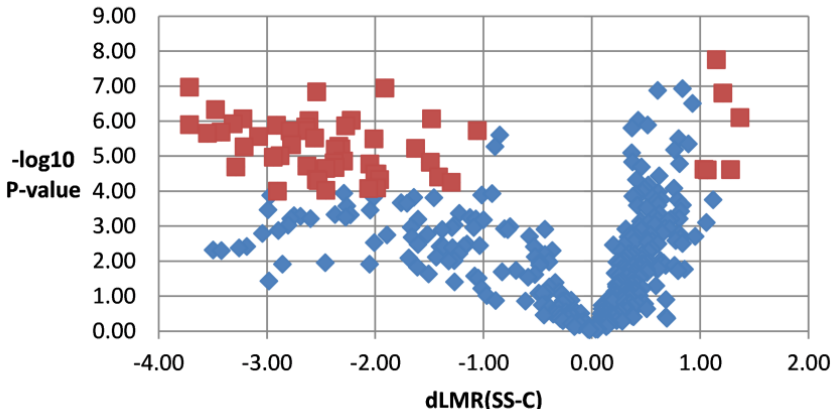

Figure 16. Scatter diagram for short DSS versus control (C) (shortened by SS-C in the figure). Significant downregulated miRNAs are shown as red plots located in the upper left part of the diagram, while the lower number of significant upregulated miRNAs are located in the upper right part. Non-significant miRNAs are illustrated as blue plots.

Table 7. The top 15 miRNAs showing largest variation in short DSS-C (shortened as SS-C in the table). Included in the table are those 15 miRNA genes with best p-values, arranged in alphabetical order.

		Average LMR		SS-C	
Annotation	p-value	SS	C	dLMR	SD dLMR
hsa-let-7b	4.75E-07	-1.438	2.037	-3.475	1.439
hsa-miR-185*	1.79E-08	0.232	-0.919	1.151	0.361
hsa-miR-191	1.37E-06	-0.696	1.578	-2.274	1.017
hsa-miR-24	8.62E-07	-1.238	1.982	-3.221	1.371
hsa-miR-26b	1.28E-06	-1.859	1.855	-3.714	1.555
hsa-miR-27b	1.07E-07	-1.801	1.914	-3.715	1.366
hsa-miR-30b	1.2E-06	-1.316	1.996	-3.312	1.362
hsa-miR-342-3p	1.48E-07	-0.880	1.659	-2.539	0.963
hsa-miR-3607-3p	9.71E-07	-0.879	1.732	-2.611	0.955
hsa-miR-3607-5p	9.6E-07	-0.650	1.572	-2.222	0.864
hsa-miR-3653	1.15E-07	-0.301	1.610	-1.911	0.714
hsa-miR-3660	1.58E-07	-0.067	-1.278	1.211	0.456
hsa-miR-552	8.01E-07	0.124	-1.246	1.369	0.584
hsa-miR-98	1.34E-06	-1.177	1.733	-2.910	1.260
hsa-miRPlus-A1015	8.68E-07	-0.269	1.211	-1.480	0.633

3.3.3 Differentially expressed miRNAs – long DSS versus control (C)

In long DSS versus C, 47 of 1274 miRNAs were significant deregulated ($p < 0.000116$, dLMR > +/- 1.0). The volcano plot is similar to that seen for short DSS-C including a majority of repressed miRNAs (Figure 17), and the top 15 miRNAs are much the same as well (Table 8).

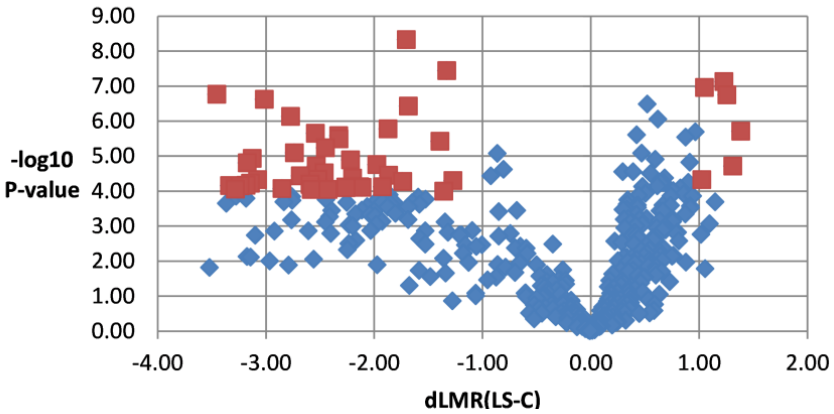

Figure 17. Volcano plot for long DSS versus control (C) (LS-C in the table). Significant downregulated miRNAs (red plots) shown in the upper left part of the diagram, while significant upregulated miRNAs (blue plots) are located in the upper right part. Non-significant miRNAs are illustrated as blue plots.

Table 8. The top 15 miRNAs showing largest variation in long DSS-C. Included in the table are those 15 miRNA genes with best p-values, arranged in alphabetical order.

		Average LMR		LS-C	
Annotation	p-value	LS	C	LS-C	LS-C
hsa-miR-126	2.42E-07	-1.141	1.873	-3.014	1.161
hsa-miR-126*	7.46E-07	-1.023	1.748	-2.770	1.065
hsa-miR-16	2.25E-06	-0.723	1.819	-2.541	1.235
hsa-miR-185*	1.8E-07	0.340	-0.919	1.259	0.462
hsa-miR-2113	1.1E-07	0.056	-0.995	1.051	0.414
hsa-miR-342-3p	3.22E-06	-0.665	1.659	-2.324	1.158
hsa-miR-3613-3p	1.72E-07	-1.444	2.009	-3.453	1.395
hsa-miR-365	2.63E-06	-0.528	1.798	-2.327	1.132
hsa-miR-3651	4.74E-09	-0.692	1.012	-1.704	0.549
hsa-miR-3653	1.67E-06	-0.263	1.610	-1.873	0.883
hsa-miR-3654	3.62E-08	-0.297	1.033	-1.330	0.480
hsa-miR-3660	7.47E-08	-0.047	-1.278	1.231	0.470
hsa-miR-4317	3.78E-06	-0.328	1.063	-1.391	0.692
hsa-miR-552	1.96E-06	0.141	-1.246	1.386	0.668
hsa-miRPlus-A1015	3.72E-07	-0.472	1.211	-1.683	0.721

3.3.4 Differentially expressed miRNAs – short DSS versus long DSS

In short DSS versus long DSS it cannot be stated significant deregulation of miRNAs, although, a number of deviant miRNAs (dLMR change > +/-0.5 (= fold change +/-1.4)) were identified (Figure 18).

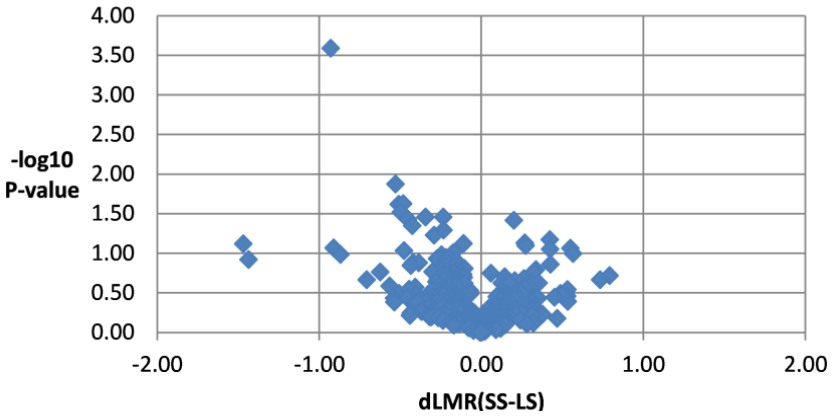

Figure 18. Volcano plot for short DSS versus long DSS. There was no significant variance in miRNA expression between short DSS and long DSS. The miRNA on top of the diagram (-log10 = 3.59) represent miR-3651, and the two miRNAs on the left miR-1290 (-log10=1.12) and miR-1246 (-log10=0.92)

3.3.5 Global miRNA expression profiling of sarcomas

Sarcoma is a rare malignancy representing diverse morphological and clinical features, meaning that performance of comprehensive miRNA profiling studies are more difficult than tumors of epithelial origin. However, there are reports in recent time describing distinct miRNA expression patterns for different types of sarcomas. In one study by Subramanian et al. 2008, miRNA screening was carried out on 27 sarcomas, five and two normal tissues of smooth muscle and skeletal muscle, respectively. Through hierarchical clustering distinct groups of LMS, SS, RMS, GIST, and normal smooth muscle were demonstrated [100]. In 2012, Renner et al. performed global expression profiling of 76 primary high-grade soft tissue sarcomas from eight different histological subtypes. In clustering analysis four main groups based on histopathological features were displayed; LMS, SS, myxoid liposarcoma, and a group containing a mix of several subtypes [101]. In both the studies, SS and LMS appeared as specific subgroups in miRNA profiling, and in this study the LMS samples were segregated. To further increase the understanding of miRNA expression in human sarcoma types it is established a database where 310 samples of 22 different tumor types have been profiled for miRNA expression. The database, named Sarcoma miRNA Expression Database (S-MED) is a public database accessible for users to identify miRNA signatures for specific sarcoma tumor types [102].

The clustering of human sarcomas in expression profiling reflects the participation of different subsets of miRNAs in tumor differentiation [100]. For example in LMS, miRNAs (miR-1, miR-133A and miR-133B) involved in myogenesis and myoblast proliferation are significant overrepresented [100]. Moreover, many sarcomas are characterized by chromosomal rearrangements of genetic material (translocations), and these are shown to be clustered together [101]. A number of sarcoma types are not categorized into groups depending on complex karyotypes leading to variable miRNA processing. Additionally, underlying molecular changes may affect the miRNA representation in some subtypes [101]. It should be mentioned that selection of normal tissue in miRNA profiling is challenging because the cells of origin are less known for some sarcoma types [103].

The current study revealed a significant number of differentially expressed miRNAs for both patient groups versus the control group, but in comparison of short and long survival of sarcoma it could not be manifested miRNAs significant for the prognosis. Other studies on carcinoma, however, have described miRNA expression relative to tumor differentiation, and the same is believed to apply for sarcoma [103]. The reason for not discover a similar trend

for the sarcoma samples could be due to limited sample number or not good enough classification of patient groups.

3.4 miR-126 expression in non-GIST STS

In the array profiling above miR-126 was identified with interesting pattern in sarcoma patients. For both miR-126 and miR-126* the experiment indicated significant downregulation in sarcoma relative to normal state. Corresponding to the non-significant results of miRNA in section 5.3.4, it was no indication of differential miR-126 expression between long DSS versus short DSS.

Table 7. Expression of miR-126/miR-126* in miRNA profiling.

	Short DSS-C		Long DSS-C		Short DSS-Long DSS	
miRNA	**dLMR**	**p-value**	**dLMR**	**p-value**	**dLMR**	**p-value**
hsa-miR-126	-2.75	0,000511	-3.01	0,000000242	-0.26	0,655
hsa-miR126*	-2.45	0,0000961	-2.77	0,000000746	-0.32	0,464

When studying the individual samples, miR-126 was found to be upregulated in three patients of short DSS in relation to the long DSS group and the control samples. Two of those were diagnosed with MFH and one with SCS. For long survival versus control, there was a consistent downregulation in all samples. The finding indicates that miR-126 may act as a suppressor in the sarcomagenesis.

3.5 miR-126 ISH in non-GIST STS

In many studies miR-126 has been found to be a particularly interesting biomarker in human cancers. Several carcinomas are characterized with reduced miR-126 expression, but enhanced expression has also been described in a less significant number of malignancies. Obviously, miR-126 contributes to tumor progression at various levels, acting both as tumor suppressors and oncogenes [61]. However, concerning the role of miR-126 in sarcomas there is only a small body of literature, and it was therefore decided to explore how miR-126 expression correlates to DSS in non-GIST STS.

In situ detection of miR-126 was carried out on the total patient cohort including samples from Norway and Russia (n=249). In order assess the real biological impact of miR-126 in

STS pathogenesis, patients with metastasis (n=43) and patients that have not undergone surgery (n=21) were excluded. Then, the initial 249 samples were reduced to 185.
The "One-day microRNA ISH protocol" (Exiqon, Denmark) was employed in the study. When staining TMA sections it is a known problem that many cores are missing or not interpretable due to technical artefacts. By including four cores of each sample, then you usually obtain sufficient and representative material for analysis of all specimens. Besides these challenges, the experiment worked well generating reliable results for samples and controls (Figure 19). In the specimens, miR-126 was expressed with various intensities in cytoplasm, and the positive U6 control displayed distinct nuclear staining. The negative scramble control was complete negative with no tendency of background staining. During the experiment there was some problem with temperature setting of the heat cabinet during SSC washing, meaning that the ISH staining for some of the TMA sections needs to be repeated to achieve intense and specific miR-126 detection in the specimens.

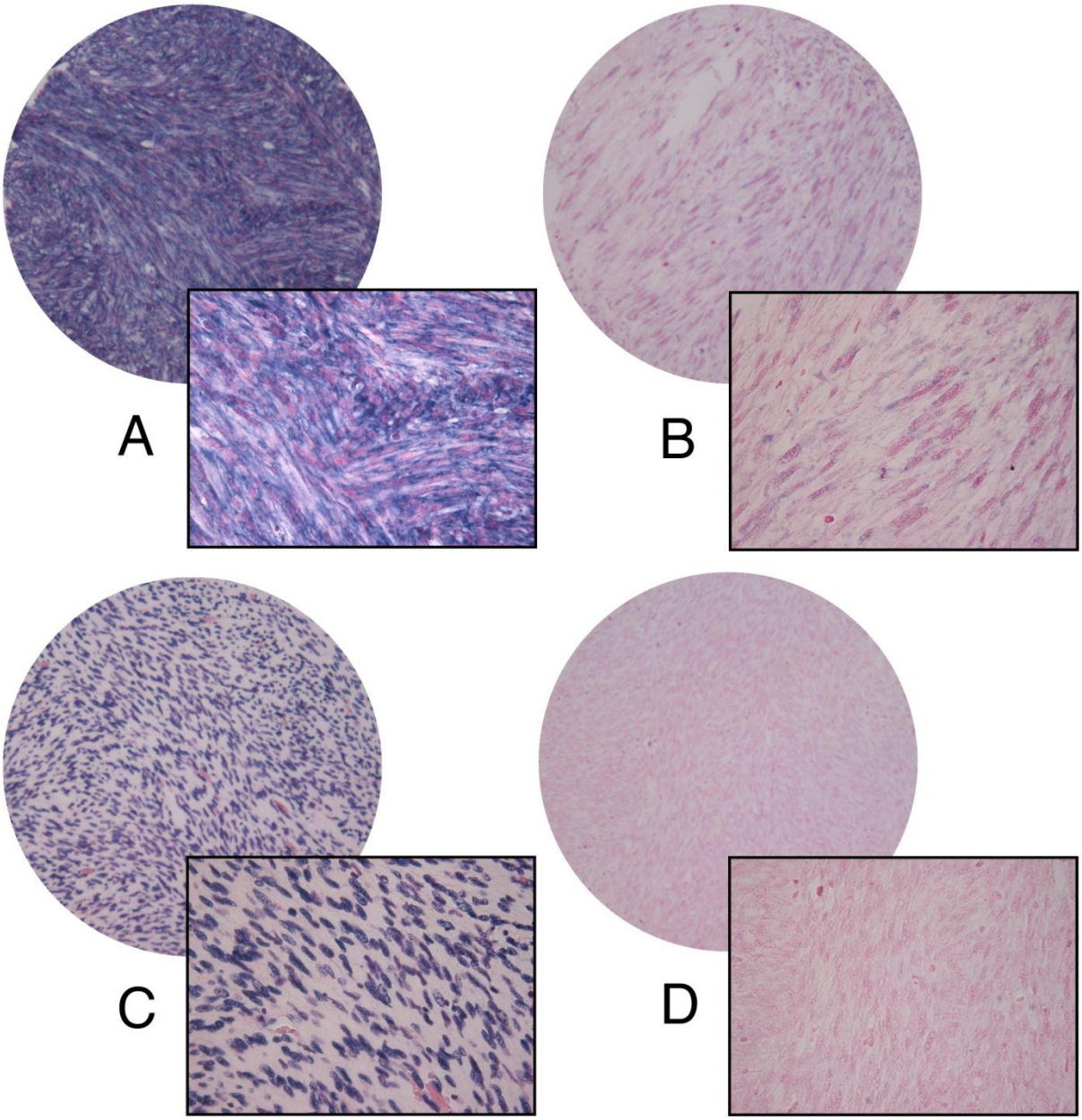

Figure 19. miRNA ISH staining, 10x and 40x objectives. A. Strong cytoplasmic staining (score 3) of miR-126 in LMS. B. Weak cytoplasmic staining (score 1) of miR-126 in LMS. C. Intense nuclear staining in the positive U6 control. D. No staining in the negative scramble control.

DSS for high and low expression of miR-126 was calculated using KM log-rank test. The cut-off value was set to 2 for discrimination between high and low expression. High scores were defined 2 and 3 and low scores 0 and 1 (Figure 19, A and B).

3.5.1 Survival assays of non-GIST STS

In survival analysis of the non-GIST STS samples (n=185) the KM log-rank test did not identify significant difference (p=0.59) between high (n=76) and low (n=109) expression of miR-126 (Figure 20). The 5-year survival rate was just under 60% regardless of miR-126 activity.

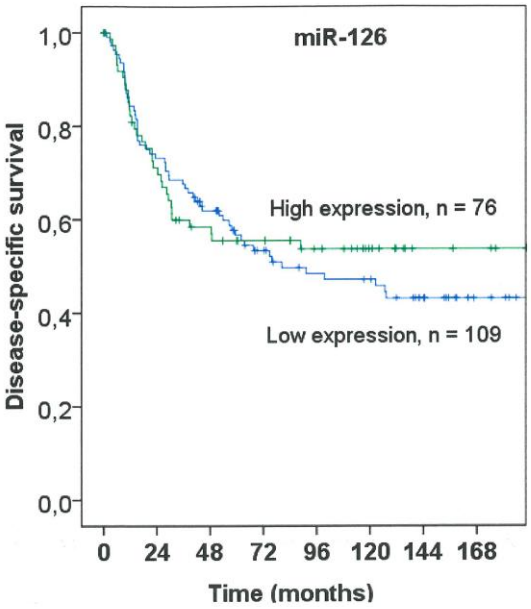

Figure 20. KM log rank test used for disease-specific survival (DSS) rate between high and low miR-126 expression in non-GIST STS. The x-axis illustrates DSS time in months, and the y-axis the fraction of cumulative survival. The cut-off value used was 2. The green curve represents the samples (n=76) with high miR-126 expression, and the blue curve the samples (n=109) with low expression. KM test did not identify significant difference (p=0.59) in survival between high and low levels of miR-126.

3.5.2 Survival assays for STS subgroups

When division into sarcoma subtypes, the disease-specific survival rate varied reflecting their histological differentiation (Table 8). In LMS, increased expression of miR-126 turned out to be a strong prognostic marker (p<0.001), and a similar, but not significant, trend was also seen in RMS (p=0.078).

Table 8. The prognostic impact of miR-126 expression (high versus low) on DSS for different histological subgroups of STSs.

Sarcoma diagnosis	Significance (p) DSS for high versus low miR-126 expression
MFH	0.259
LMS	0.000
Liposarcoma	0.324
Fibrosarcoma	0.752
Angiosarcoma	0.177
RMS	0.078
SS	0.453

3.5.3 Survival assays for LMS

Survival analysis of LMS samples clearly indicates that people with high miR-126 expression has better prognostic outcome than patients with low expression. For those with high levels (n=19) the relative 5-year survival rate was around 90%, and 40% for those with low levels (n=26), but dropped to 20% for patients living longer 10 years following diagnosis (Figure 21). Despite the limited sample material, the results demonstrate the strong influence of miR-126 expression on prognosis for LMS patients.

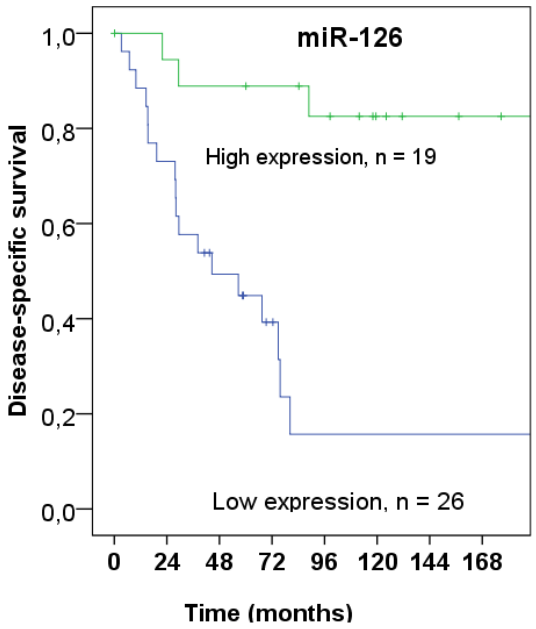

Figure 21. KM log rank test for DSS rate between high and low expression of miR-126 in LMS samples. For people with high miR-126 expression (n=19, green curve) the 10-year survival rate was just above 80%, and for patients with low expression (n=26, blue curve) the 10-year survival rate was 20% (p<0.001).

3.5.4 Survival analyses of uterus LMS versus non-uterus LMS

The impact of miR-126 on LMS was further investigated through splitting into uterus and non-uterus subgroups. For uterus-LMS the relative 5-year survival rate was 80% for patients with high miR-126 expression (n=10) and approximately 30% for those with low expression (n=12) (Figure 22). The prognostic significance was p<0.018.

For non-uterus LMS the results were quite remarkable. People with high levels of miR-126 (n=9) the survival rate was 100%, but for those with low levels (n=14) all suffers a sarcoma-related death (Figure 23). The differentiated behavior of miR-126 in LMS subgroups can be explained by the fact that uterus-LMS derives from myometrium and non-uterus LMS from smooth muscle of large vessels [100].

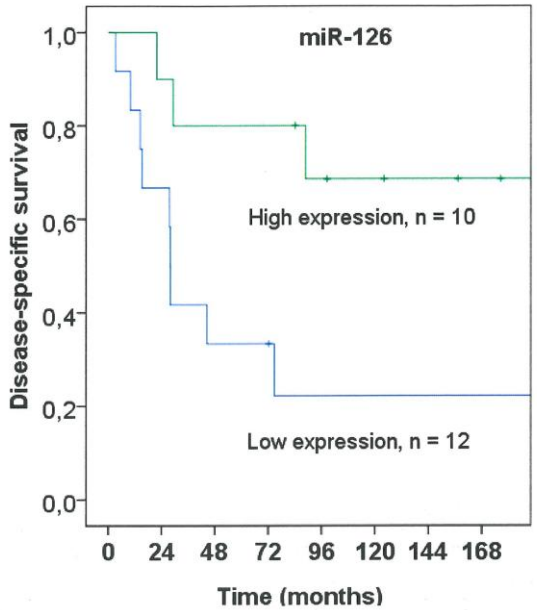

Figure 22. KM log rank test for DSS rate between high and low expression of miR-126 in uterus LMS. For people with high miR-126 expression (n=10, green curve) the 10-year survival rate was around 70%, and for patients with low expression (n=12, blue curve) the 10-year survival rate was 20% (p<0.018).

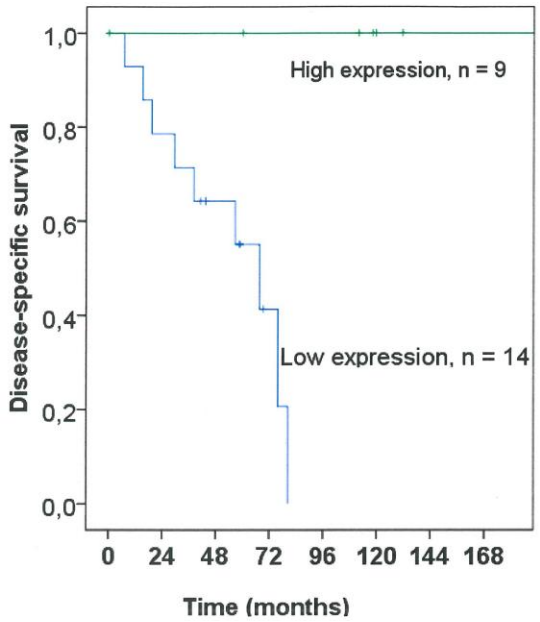

Figure 23. KM log rank test used for DSS rate between high and low expression of miR-126 in non-uterus LMS. For people with high miR-126 expression (n=9, green curve) the 10-year survival rate was 100%, and for patients with low expression (n=14, blue curve) the 10-year survival rate was zero (p<0.001).

3.5.5 miR-126 as a prognostic marker in LMS

As discussed above, miR-126 has been found to be a key factor in initiation and progression of several cancers. Depending on type of tumor tissue miR-126 bind different target genes determining cell fate mechanisms, including proliferation, migration, and invasion [104-106]. Declining miR-126 expression is believed to stimulate the aggressiveness of tumors through larger tumor size, deeper invasion, lymph node metastasis, and advanced TNM staging. Conversely, it is found that transfection of miR-126 precursors into cultured cell lines inhibits the growth and malignant potential of tumor cells [107].

In sarcomas, the role of miR-126 is less well understood. In a review by Drury et al. 2012, expression data from several profiling studies on sarcomas show upregulation of miR-126 in osteosarcoma and Ewing sarcoma [103]. In the present study the biological impact of miR-126 in non-GIST STS is variable. For LMS miR-126 turned out to be an important tumor marker, and for LMS of non-uterus origin the significance became even stronger. But, the rest of STSs appeared not to be affected as much by deviant miR-126 expression, except for a weak tendency in RMS. A profiling study of LMS in 2010 observed miR-126 as a critical factor in smooth muscle differentiation and LMS development. Their data demonstrated significant downregulation of miR-126 in LMS tumors relative to benign uterine smooth muscle or myometrium [108].

LMS is known as a highly aggressive tumor with poor prognosis, and because of the few cases (0.7% of all cancers, 5-10% of STSs) and its heterogenous appearance, it makes it difficult to implement distinct studies [108, 109]. Today, there are some studies identifying specific miRNAs misexpressed in LMS, however, better understanding of the molecular mechanism is essential to improve the prognosis for people suffered by the disease [103, 108].

Conclusion

In recent years miRNAs have emerged as critical players in development of human cancers. Several carcinomas have been characterized with unique miRNA patterns that might be useful in tumor classification and prognosis. Concerning the influence of miRNA transcripts in sarcomas, the knowledge is considerably less. Therefore, it was decided to explore the role of miRNAs in non-GIST soft tissue sarcomas, both at global level in different prognostic groups and for specific miRNA in DSS subgroups.

The total sample material included 249 non-GIST STS patients diagnosed at UNN and hospitals in Arkhangelsk County, Russia. The sample material consisting of FFPE biopsies were retrieved from the respective histological archives. To enable high throughput analysis under identical and standardized conditions TMA cohorts were established. The strategy to identify prognostic miRNAs in soft tissue sarcomas involve microarray-based miRNA expression profiling of a selected number of specimens based on disease outcome. Two patient groups representing long DSS (n=11) and short DSS (n=10) mainly diagnosed with LMS and MFH, and a control (C) group (n=10) of benign connective tissue were included. In global expression profiling of all human, mouse, and rat miRNAs registered in miRBase version 16 (n=1274), 54 miRNAs in long DSS and 47 miRNAs in short DSS turned out to be significant deregulated when comparing to Cs, and a majority of these were suppressed. Many of these miRNAs are known from the literature as crucial regulators of cellular processes and associated with human cancers.

For long DSS versus short DSS it could not be manifested significant differentiation in miRNA regulation. Aberrant miRNA expression correlating to tumor grade has been described in carcinomas, but has not been discussed to the same extent in sarcoma studies. Whether there is an underlying trend of miRNA levels corresponding to prognosis in non-GIST STS that was not detected, it could be due to limited sample material included or not good enough division of prognostic groups. Additionally, the heterogenous histological characteristics increased the risk of getting negative results.

In the screening, the angiogenic related miR-126 was strongly downregulated in long DSS and short DSS compared to C. Its biological impact on non-GIST STS was studied through *in situ* hybridization of the total patient cohort. In survival analysis including all histological subgroups the Kaplan-Meier log-rank test did not identify significant differentiation (p=0.59) between high and low expression of miR-126. But, when stratifying for different histological subtypes there were variances in survival rate based on miR-126 expression. For LMS it was

an evident difference ($p<0.001$) in the prognostic outcome between patients with high and low expression of miR-126, and to some extent for RMS ($p=0.078$). In the rest of subgroups the level of miR-126 expression did not affect the prognosis. In LMS patients with high levels of miR-126 the relative five-year survival rate was approximately 90%, and for low levels around 40%, declining to 20% the next five years. When splitting LMS into uterus and non-uterus subgroups, it was shown that the prognostic significance of miR-126 became even stronger in the non-uterus cases. For high expression the survival rate was 100%, and for low expression no one survived.
Although the limited sample material, these findings indicate the crucial role of miR-126 in LMS. To further validate the biological impact of miR-126 it is necessary include cohorts of more LMS cases, and to compare with other methodologies, such as real-time PCR and cultured cell lines. Then, if the validation generates substantial results miR-126 could be established in diagnostic and clinical settings.

In a future perspective, this study and widely research demonstrate the potential of miRNAs as powerful biomarkers in cancer diagnostics. Use of miRNA expression profiling might provide opportunities to improve the subclassification of tumors and prognosis. Moreover, miRNAs can be used in development of effective treatment strategies.

Considering the practical performance of the miRNA ISH experiment, the protocol used was found to be robust and reliable in detection of cytoplasmic miR-126 expression in tissue samples. The experiment demonstrated that *in situ* hybridization is an excellent approach to study miRNA expression in single cells, and can advantageously be used in routine diagnostics. But one should keep in mind that ISH staining is not an ideal method for absolute quantification of miRNA levels in a biological context. In that sense real-time PCR is a better option.

Reference List

[1] http://www.cancer.org/cancer/cancerbasics/what-is-cancer. 2013.

[2] http://cancer.stanford.edu/information/geneticsAndCancer/genesCause.html. 2013.

[3] Hanahan D, Weinberg RA. Hallmarks of cancer: the next generation. Cell 2011;144:646-74.

[4] Baba AI, Catoi C. 2007.

[5] http://www.webmd.com/cancer/understanding-cancer-basics. 2013.

[6] http://www.cancer.net/all-about-cancer/risk-factors-and-prevention/understanding-cancer-risk. 2013.

[7] http://www.who.int/dg/speeches/2010/iaea_forum_20100921/en/. 2013.

[8] http://en.wikipedia.org/wiki/Sarcoma. 2013.

[9] Janeway KA. New strategies in sarcoma therapy: linking biology and novel agents. 2012.

[10] http://cancer.northwestern.edu/cancertypes/cancer_type.cfm?category=23. 2013.

[11] http://www.seattlecca.org/diseases/types-subtypes-sarcoma.cfm. 2013.

[12] http://sarcomaoncology.com/s_as_sarcoma.html. 2013.

[13] Wolden SL, Alektiar KM. Sarcomas across the age spectrum. Semin Radiat Oncol 2010;20:45-51.

[14] Pike JCPWMBA. Soft tissue sarcomas of the extremities: How to stay out of trouble. BCMJ 2008;50:310-7.

[15] http://www.cancer.net/cancer-types/sarcoma/symptoms-and-signs. 2013.

[16] http://www.cancer.net/cancer-types/sarcoma/diagnosis. 2013.

[17] Hornick JL. The prognostic role of immunohistochemistry in sarcomas. 2010.

[18] Wardelmann E, Schildhaus HU, Merkelbach-Bruse S, et al. Soft tissue sarcoma: from molecular diagnosis to selection of treatment. Pathological diagnosis of soft tissue sarcoma amid molecular biology and targeted therapies. Ann Oncol 2010;21 Suppl 7:vii265-vii269.

[19] Tschoep K, Kohlmann A, Schlemmer M, Haferlach T, Issels RD. Gene expression profiling in sarcomas. Crit Rev Oncol Hematol 2007;63:111-24.

[20] Carvajal RD. http://emedicine.medscape.com/article/2006584-overview. 2013.

[21] Hoppin JA, Tolbert PE, Flanders WD, et al. Occupational risk factors for sarcoma subtypes. Epidemiology 1999;10:300-6.

[22] Thagian A, de Vathaire F, Terrier P. Long-term risk of sarcoma following radiation treatment for breast cancer. Int J Radiat Oncol Biol Phys 1991;21:361-7.

[23] http://www.cancer.gov/cancertopics/pdq/treatment/adult-soft-tissue-sarcoma/Patient/page1. 2013.

[24] http://www.cancer.org/cancer/sarcoma-adultsofttissuecancer/detailedguide/sarcoma-adult-soft-tissue-cancer-treating-by-stage. 2013.

[25] Siehl J, Thiel E. C-kit, GIST, and imatinib. Recent Results Cancer Res 2007;176:145-51.

[26] http://www.cancer.org/cancer/sarcoma-adultsofttissuecancer/detailedguide/sarcoma-adult-soft-tissue-cancer-survival-rates. 2013.

[27] Bartel DP. MicroRNAs: genomics, biogenesis, mechanism, and function. 2004.

[28] Siomi H, Siomi MC. Posttranscriptional regulation of microRNA biogenesis in animals. Mol Cell 2010;38:323-32.

[29] Sun W, Julie Li YS, Huang HD, Shyy JY, Chien S. microRNA: a master regulator of cellular processes for bioengineering systems. Annu Rev Biomed Eng 2010;12:1-27.

[30] He L, Hannon GJ. MicroRNAs: small RNAs with a big role in gene regulation. Nat Rev Genet 2004;5:522-31.

[31] Berezikov E, Cuppen E, Plasterk RH. Approaches to microRNA discovery. Nat Genet 2006;38 Suppl:S2-S7.

[32] ftp://mirbase.org/pub/mirbase/CURRENT/README. 2013.

[33] Park K, Kim KB. miRTar Hunter: a prediction system for identifying human microRNA target sites. Mol Cells 2013;35:195-201.

[34] Davis-Dusenbery BN, Hata A. Mechanisms of control of microRNA biogenesis. J Biochem 2010;148:381-92.

[35] Visone R, Croce CM. MiRNAs and cancer. Am J Pathol 2009;174:1131-8.

[36] http://en.wikipedia.org/wiki/Piwi-interacting_RNA. 2013.

[37] http://en.wikipedia.org/wiki/Small_interfering_RNA. 2013.

[38] http://en.wikipedia.org/wiki/MicroRNA. 2013.

[39] http://www.mirbase.org/help/nomenclature.shtml. 2013.

[40] Kim VN. Genomics of microRNA. 2006.

[41] Lee Y, Kim M, Han J, et al. MicroRNA genes are transcribed by RNA polymerase II. EMBO J 2004;23:4051-60.

[42] Winter J, Jung S, Keller S, Gregory RI, Diederichs S. Many roads to maturity: microRNA biogenesis pathways and their regulation. Nat Cell Biol 2009;11:228-34.

[43] Tomari Y, Zamore PD. MicroRNA biogenesis: drosha can't cut it without a partner. Curr Biol 2005;15:R61-R64.

[44] Kim VN. MicroRNA biogenesis: coordinated cropping and dicing. Nat Rev Mol Cell Biol 2005;6:376-85.

[45] Meltzer PS. Small RNAs with big impacts. Nature News & Views 2005;435:745-6.

[46] Cai Y, Yu X, Hu S, Yu J. A brief review on the mechanism of miRNA regulation. Genomics Proteomics Bioinformatics 2009;7:147-54.

[47] Krol J, Loedige I, Filipowicz W. The widespread regulation of microRNA biogenesis, function and decay. Nat Rev Genet 2010;11:597-610.

[48] Wang J, Lu M, Qiu C, Cui Q. TransmiR: a transcription factor-microRNA regulation database. Nucleic Acids Res 2010;38:D119-D122.

[49] http://cmbi.bjmu.edu.cn/transmir. 2013.

[50] Han J, Pedersen JS, Kwon SC, et al. Posttranscriptional crossregulation between Drosha and DGCR8. Cell 2009;136:75-84.

[51] Blow MJ, Grocock RJ, van DS, et al. RNA editing of human microRNAs. Genome Biol 2006;7:R27.

[52] Sato F, Tsuchiya S, Meltzer SJ, Shimizu K. MicroRNAs and epigenetics. FEBS J 2011;278:1598-609.

[53] Chuang JC. Epigenetics and microRNAs. 2007.

[54] Farazi TA, Spitzer JI, Morozov P, Tuschl T. miRNAs in human cancer. J Pathol 2011;223:102-15.

[55] Sassen S, Miska EA, Caldas C. MicroRNA: implications for cancer. Virchows Arch 2008;452:1-10.

[56] Calin GA, Croce CM. MicroRNA signatures in human cancers. Nat Rev Cancer 2006;6:857-66.

[57] Garzon R, Calin GA, Croce CM. MicroRNAs in Cancer. Annu Rev Med 2009;60:167-79.

[58] Esquela-Kerscher A, Slack FJ. Oncomirs - microRNAs with a role in cancer. Nat Rev Cancer 2006;6:259-69.

[59] Rouhi A, Mager DL, Humphries RK, Kuchenbauer F. MiRNAs, epigenetics, and cancer. Mamm Genome 2008;19:517-25.

[60] Sun Y, Bai Y, Zhang F, Wang Y, Guo Y, Guo L. miR-126 inhibits non-small cell lung cancer cells proliferation by targeting EGFL7. Biochem Biophys Res Commun 2010;391:1483-9.

[61] Meister J, Schmidt MH. miR-126 and miR-126*: new players in cancer. ScientificWorldJournal 2010;10:2090-100.

[62] Li N, Tang A, Huang S, et al. MiR-126 suppresses colon cancer cell proliferation and invasion via inhibiting RhoA/ROCK signaling pathway. Mol Cell Biochem 2013;380:107-19.

[63] Wang S, Aurora AB, Johnson BA, et al. The endothelial-specific microRNA miR-126 governs vascular integrity and angiogenesis. Dev Cell 2008;15:261-71.

[64] Nikolic I, Plate KH, Schmidt MH. EGFL7 meets miRNA-126: an angiogenesis alliance. J Angiogenes Res 2010;2:9.

[65] Harris TA, Yamakuchi M, Kondo M, Oettgen P, Lowenstein CJ. Ets-1 and Ets-2 regulate the expression of microRNA-126 in endothelial cells. Arterioscler Thromb Vasc Biol 2010;30:1990-7.

[66] Fish JE, Santoro MM, Morton SU, et al. miR-126 regulates angiogenic signaling and vascular integrity. Dev Cell 2008;15:272-84.

[67] Hoos A, Cordon-Crado C. Tissue microarray profiling of cancer specimens and cell lines: opportunities and limitations. Lab Invest 2001;81:1331-8.

[68] Nazar MT. Tissue Microarray: A rapidly evolving diagnostic and research tool. Ann Saudi Med 2009;29:123-7.

[69] http://sunnybrook.ca/research/content/?page=sri-core-genom-equip-8. 2013.

[70] Beecher Instruments Inc SPWU. Instruction manual, Micro Tissue Arrayer (MTA-1). 1998.

[71] Parsons M, Grabsch H. How to make tissue microarrays. Diagnostic Histopathology 2009;15:142-50.

[72] Liu CG, Calin GA, Volinia S, Croce CM. MicroRNA expression profiling using microarrays. Nat Protoc 2008;3:563-78.

[73] Murphy D. Gene expression studies using microarrays:principles, problems, and prospects. Adv Physiol Edu 2 A.D.;26:256-70.

[74] Kong W, Zhao JJ, He L. Strategies for profiling microRNA expression. J Cell Physiol 2009;218:22-5.

[75] Lu J, getz g, Miska EA. MicroRNA expression proiles classify human cancers. Nature 2005;435.

[76] Cummins JM, Velculescu VL. Implications of micro-RNA profiling for cancer diagnosis. Oncogene 2006;25:6220-7.

[77] Pritchard CC, Cheng HH, Tewari M. MicroRNA profiling: approaches and considerations. Nat Rev Genet 2012;13:358-69.

[78] Exiqon AS VD. miRCURY LNA™ microRNA Array Kit 6th generation - human mouse & rat . 2013.

[79] Exiqon A/S VD. MicroRNA Array Final Service Report. 2011 Feb 1.

[80] Roberts P. MicroRNA expression profiling on arrays enhanced with locked nucleic acids. Nature Methods 2006.

[81] Koshkin AA, Singh SK, Nielsen P, et al. LNA (Locked Nucleic Acids): Synthesis of the adenine, cytosine, guanine, 5-metylcytosin, thymine and uracil bicyclonucleoside monomers, oligomerisation and unprecedented nucleic acid recognition. Tetrahedron 1998;54:3607-30.

[82] http://www.exiqon.com/lna-technology. 2013.

[83] http://www.sigmaaldrich.com/life-science/custom-oligos/dna-probes/product-lines/lna-probes/locked-nucleic-acids-faq.html. 2013.

[84] Sreekumar JJKK. Statistical tests for identification of differentially expressed genes in cDNA microarray experiments. Indian Journal of Biotechnology 2008;7:423-36.

[85] Meyer SU, Pfaffl MW, Ulbrich SE. Normalization strategies for microRNA profiling experiments: a 'normal' way to a hidden layer of complexity? Biotechnol Lett 2010;32:1777-88.

[86] Yin JQ, Zhao RC, Morris KV. Profiling microRNA expression with microarrays. Trends Biotechnol 2008;26:70-6.

[87] Wilcox JN. Fundamental principles of in situ hybridization. J Histochem Cytochem 1993;41:1725-33.

[88] Nelson PT. RAKE and LNA-ISH reveal microRNA expression and localization in archival human brain. 2006.

[89] Nielsen BS. MicroRNA In Situ Hybridization. 2012.

[90] Jorgensen S, Baker A, Moller S, Nielsen BS. Robust one-day in situ hybridization protocol for detection of microRNAs in paraffin samples using LNA probes. Methods 2010;52:375-81.

[91] Bernardo BC, Charchar FJ, Lin RC, McMullen JR. A microRNA guide for clinicians and basic scientists: background and experimental techniques. Heart Lung Circ 2012;21:131-42.

[92] Exiqon AS VD. miRCYRY LNA™ microRNA ISH Optimization Kit (FFPE) Instruction manual v2.0. 2013.

[93] Valkov A, Kilvaer TK, Sorbye SW, et al. The prognostic impact of Akt isoforms, PI3K and PTEN related to female steroid hormone receptors in soft tissue sarcomas. J Transl Med 2011;9:200.

[94] Valkov A. Molecular prognostic markers in soft tissue sarcomas. 2012 Sep.

[95] Ambion RNA lt. RecoverAll™ Total Nucleic Acid Isoalation Kit . 2011.

[96] www.u.arizona.edu/~gwatts/.../InterpretingSpec.pdf? 2013 Dec.

[97] Pedersen M, Eklo. miRNA ISH protocol at UiT. 2011.

[98] http://technoinfo.co.uk/catalog/14.html. 2014.

[99] Ariol scanning procedure. 2014.

[100] Subramanian S, Lui WO, Lee CH, et al. MicroRNA expression signature of human sarcomas. Oncogene 2008;27:2015-26.

[101] Renner M, Czwan E, Hartmann W, et al. MicroRNA profiling of primary high-grade soft tissue sarcomas. Genes Chromosomes Cancer 2012;51:982-96.

[102] Sarver AL, Phalak R, Thayanithy V, Subramanian S. S-MED: sarcoma microRNA expression database. Lab Invest 2010;90:753-61.

[103] Drury R, Verghese ET, Hughes TA. The roles of microRNAs in sarcomas. J Pathol 2012;227:385-91.

[104] Zhang J, Du YY, Lin YF, et al. The cell growth suppressor, mir-126, targets IRS-1. Biochem Biophys Res Commun 2008;377:136-40.

[105] Sun Y, Bai Y, Zhang F, Wang Y, Guo Y, Guo L. miR-126 inhibits non-small cell lung cancer cells proliferation by targeting EGFL7. Biochem Biophys Res Commun 2010;391:1483-9.

[106] Hamada S, Satoh K, Fujibuchi W, et al. MiR-126 acts as a tumor suppressor in pancreatic cancer cells via the regulation of ADAM9. Mol Cancer Res 2012;10:3-10.

[107] Feng R, Chen X, Yu Y, et al. miR-126 functions as a tumour suppressor in human gastric cancer. Cancer Lett 2010;298:50-63.

[108] Danielson LS, Menendez S, Attolini CS, et al. A differentiation-based microRNA signature identifies leiomyosarcoma as a mesenchymal stem cell-related malignancy. Am J Pathol 2010;177:908-17.

[109] Weaver MJ, Abraham JA. Leiomyosarcomas of the bone and soft tissue: A review. 2007.